Faraday Discuss. Chem. Soc., 1987, **84**, 87–126

GENERAL DISCUSSION

Prof. J. N. Murrell (*University of Sussex*) said: The experimental results presented by Robinson, Continetti and Lee are startling and if confirmed would have a substantial impact on our understanding of radical substitution reactions of aromatic molecules. For radical reactions in solution alkyl substituents have a very weak directing effect, and indeed in the paper it is recognised that both the endothermicity, and the energy of any intermediate complex, are little affected by the methyl group. The authors therefore attribute the non-reactivity of the *meta* isomer, and, as reported in the discussion, the non-reactivity of chlorobenzene itself, to subtleties in the shapes of the exit valleys of the reactions. If this were true we would be introducing new criteria into the theory of organic reactivity, and before going down that path it would seem wise to carry out other experiments, *e.g.* molecular beam studies of the reverse reactions.

Mr G. N. Robinson, Mr R. E. Continetti and **Prof. Y. T. Lee** (*University of California, Berkeley, CA*) said: In reply to Prof. Murrell, our experimental results were reproduced several times and the difference in cross-section that we observed between the *meta* isomer and the *ortho* and *para* isomers is certainly real. Concerning any disagreements between our results and those of previous experiments on aromatic substitution in solution, we would simply observe that an experiment that measures relative rates of homolytic or ionic substitution in solution will not be sensitive to features of the reactive potential-energy surface in the way that a scattering experiment is. We are contemplating a series of experiments to investigate further the effects of substituents on the dynamics of aromatic substitution reactions.

Prof. R. N. Zare (*Stanford University, CA*) said: I found this crossed-molecular-beam study of aromatic substitution reaction to be most fascinating and to raise a number of questions:

(1) Was a study made of the reverse reaction, Cl + *o*-,*m*-,*p*-bromotoluene? What can your present results tell us to expect about this reverse reaction?

(2) When fast Br atoms encounter *o*-,*m*-,*p*-chlorotoluene is HBr production observed? If not, is it understood why this reaction channel is unimportant?

(3) In the Br + *o*-,*p*-chlorotoluene substitution reaction, the product angular distribution and time-of-flight spectra are fit assuming that a limited number of oscillators in the complex are excited, *i.e.* participate in the energy sharing prior to Cl atom elimination. Is it known which oscillators are involved? Have studies been made with Br and fully or partially deuterated *o*-,*p*-chlorotoluene?

(4) What role does the methyl group play in affecting the observed differences between *ortho* and *para* chlorotoluene? Are there both electronic and steric effects? Have corresponding studies been made on *o*-,*p*-chloroaniline and on *o*-,*p*-chlorophenol?

Mr G. N. Robinson, Mr R. E. Continetti and **Prof. Y. T. Lee** (*University of California, Berkeley, CA*) said in reply to Prof. Zare:

(1) We did not investigate the reactions Cl + *o*-,*m*-,*p*-bromotoluene → Br + *o*-,*m*-,*p*-chlorotoluene. On the basis of the reasoning proposed near the end of our paper, we believe that the reactions Cl + *o*-,*p*-bromotoluene will have higher cross-sections than Cl + *m*-bromotoluene. Since ΔH° for the isomeric Br + chlorotoluene reactions are nearly the same, ΔG° and K_{eq} are also likely to be the same. Therefore, if the rate constant for the reaction in the endoergic direction is large, the rate constant for the reverse, exoergic reaction should also be large.

(2) The H-atom abstraction reactions ($Br + C_7H_7Cl \rightarrow HBr + C_7H_6Cl$) were not studied because there would be substantial background at both product masses at all laboratory angles from inelastic/elastic scattering of the reagents. It is worth considering the energetics of these reactions, however. Abstraction of a ring H atom by Br is endoergic by 24 kcal mol^{-1}. An additional barrier of *ca.* 10 kcal mol^{-1} (which is not unlikely) would prevent this reaction from occurring at the highest collision energy of our experiments. Yet, even if H abstraction had the same energetic threshold as Cl substitution, direct abstraction would probably occur less readily than Cl substitution since the relative energy of a binary Br—H collision is 49 times smaller than that for Br + CT. Br addition and subsequent HBr elimination would be a more likely way to form HBr with a ring H atom.[1] Overall, direct abstraction of a benzylic H atom would be the more likely reaction to form HBr since it is exoergic by 2 kcal mol^{-1}. The activation energy for the reaction $Br + C_6H_5\text{-}CH_3 \rightarrow HBr + C_6H_5\text{-}CH_2$ is known to be 7.2 kcal mol^{-1}.[2]

(3) We have not studied the Br + chlorotoluene reactions with deuterated compounds although the lower frequency of the C-C-D bending modes might have an effect on the observed dynamics. We *have* studied the reactions $Br + C_6X_5Cl \rightarrow C_6X_5Br + Cl$ (X = H, F).[3] At a collision energy of *ca.* 30 kcal mol^{-1} no substitution product is observed for X = H whereas substitution product *is* observed for X = F. We attribute this difference in reactivity to a larger addition cross-section for $Br + C_6F_5Cl$. Both the product translational energy distributions and the excitation function for $Br + C_6F_5Cl \rightarrow Cl + C_6F_5Br$ suggest that a larger number of modes participate in energy sharing in this reaction than in the chlorotoluene reactions.

In none of these reactions can we actually identify the modes involved and we do not maintain that there is a microcanonical equilibrium among a fixed number of modes prior to bond breakage. In fact IVR competes with bond breakage in these reactions. Our value for the number of active modes is then a relative measure of the extent to which energy is drained away from the reaction coordinate prior to bond breakage. A small point: in fitting our data we used parametrized functions for the c.m. frame flux distribution and assumed nothing about the extent of energy redistribution in the BCMC complexes. The best-fit $P(E')$ for the Br + *o*-chlorotoluene reaction at 31.5 kcal mol^{-1} was compared to RRKM-AM $P(E')$ distributions that were calculated for different numbers of active modes.

(4) It is certainly possible that factors other than those discussed in our paper contribute to the observed difference between the *o*-and *p*-bromotoluene excitation functions. The heats of formation of the BC2MC and BC4MC radicals, however, are unlikely to be different from one another. We base this conclusion on an assessment of the relative heats of formation of the (hypothetical) conjugated radicals formed when the halogenated carbon atom is removed from the ring, *i.e.* the 1-methylpentadienyl and 4-methylpentadienyl radicals. Although there appear to be no ΔH_f° data for these radicals, there are ΔH_f° values for the methylallyl and 2-methylallyl radicals.[4] Within experimental error these values are the same (30.0 kcal mol^{-1}). Subtle differences between the slopes of the Br + *o*-CT and *p*-CT potential energy surfaces along the reaction coordinate cannot be ruled out however.

The methyl group may indeed block Br addition to the chlorinated carbon of *o*-chlorotoluene at low collision energies causing $S_{r,o\text{-bromotoluene}}$ to be lower than $S_{r,p\text{-bromotoluene}}$ for $E_c < 25$ kcal mol^{-1}. With the number of dissipative modes in the vicinity of the collision being larger for *o*-chlorotoluene, σ_{add}(*o*-chlorotoluene) may be higher than σ_{add}(*p*-chlorotoluene) for $E_c > 25$ kcal mol^{-1}. The increased sideways scattering that we observe for the *o*-chlorotoluene reaction at higher collision energies is consistent with wider angle Br + *o*-chlorotoluene collisions becoming reactive as the collision energy is raised.

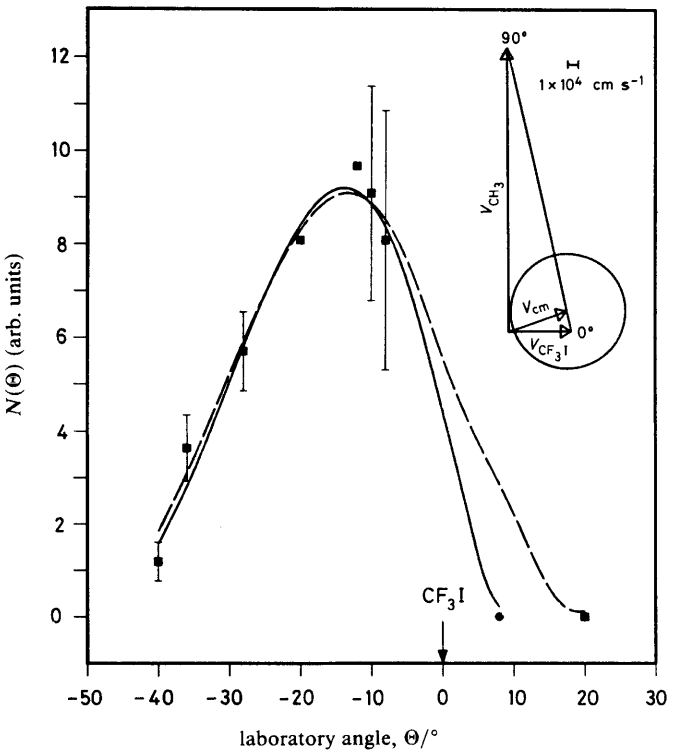

Fig. 1. CH_3I ($m/e = 142$) laboratory angular distribution from the reaction $CH_3 + CF_3I \rightarrow CH_3I + CF_3$, $E_c = 12$ kcal/mol. Solid and dashed lines are fits to data using the solid and dashed line $T(\theta)$ distributions in fig. 2(*a*) and the $P(E')$ in fig. 2(*b*). Radius of Newton circle represents the maximum CH_3I recoil velocity in the c.m. frame.

Finally, no studies have been carried out with OH and NH_2 substituted compounds, although their *ortho-para*-directing effects should be greater than that for CH_3. Future investigations of substituent effects are planned.

1 A. S. Rodgers, D. M. Golden and S. W. Benson, *J. Am. Chem. Soc.*, 1967, **89**, 4578.
2 H. R. Anderson Jr, H. A. Scheraga and E. R. VanArtsdalen, *J. Chem. Phys.*, 1953, **21**, 1258
3 G. N. Robinson, R. E. Continetti and Y. T. Lee, to be published.
4 D. F. McMillan and D. M. Golden, *Annu. Rev. Phys. Chem.*, 1982, **33**, 493.

Mr G. N. Robinson, Dr G. M. Nathanson, Mr R. E. Continetti and **Prof. Y. T. Lee** (*University of California, Berkeley, CA*) said: We have carried out a crossed beam study of the iodine exchange reaction, $CH_3 + CF_3I \rightarrow CH_3I + CF_3$ ($-\Delta H° \approx 0$–2 kcal mol^{-1}), at a collision energy of *ca.* 12 kcal mol^{-1}. We generate a supersonic methyl radical beam in a manner similar to that of Grice and co-workers[1c] by passing a mixture of *ca.* 2% di-t-butyl peroxide in He through a quartz nozzle (0.5 mm diameter) that is in contact with a resistively heated tantalum strip. The nozzle temperature is *ca.* 1000 °C. A laboratory CH_3I product angular distribution ($m/e = 142$) is shown in fig. 1. The angle at which the distribution falls to zero for $\Theta > 0°$ is uncertain because of the presence of background at these angles caused by in/elastically scattered impurity from the CF_3I beam. Although it is certain that $N(20°) = 0$, it is likely that $N(8°) = 0$ ($\Theta_{cm} = 19°$). The angular distributions and time-of-flight data (not presented) are fitted with the c.m. frame product angular and translational energy distributions shown in fig. 2. $P(E')$ distributions having thresholds in the range 0–3 kcal mol^{-1} can fit the data.

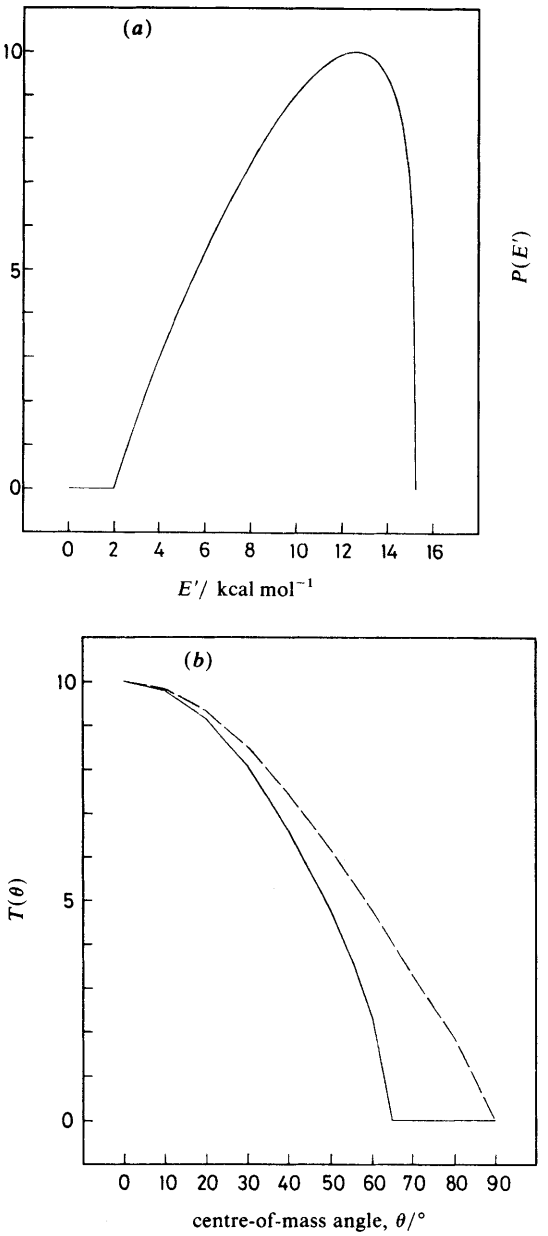

Fig. 2. (*a*) Centre-of-mass (c.m.) frame product relative translational energy distribution for $CH_3+CF_3I \rightarrow CH_3I+CF_3$, $E_c = 12$ kcal mol^{-1}. (*b*) CH_3I c.m. frame angular distributions; see fig. 1.

The high average product translational energy, $\langle E'/E_{avl}\rangle = 0.66$, and sharp backward scattering of the CH_3I product indicates that a roughly collinear $CH_3—I—CF_3$ geometry is favoured. The fraction of available energy that is channelled into translation is greater than that for the $CH_3+IY \rightarrow CH_3I+Y$ (Y=Cl, Br, I) reactions, where $\langle E'/E_{avl}\rangle \approx 0.3$,[1] suggesting that the CH_3+CF_3I potential-energy surface is more repulsive in its exit

valley than the $CH_3—I—Y$ surfaces. In addition, the vibrational modes of the CF_3 group appear to play a very limited role in product energy partitioning for this reaction. This may be partly due to the similarity in structure of the CF_3 groups in CF_3I and CF_3. Finally, these results are remarkably similar to those obtained by Davidson *et al.*[2] for the reaction $D+CF_3I \rightarrow DI+CF_3$ where the DI product was strongly backward scattered and $\langle E'/E_{avl}\rangle \approx 0.7$.

1 (*a*) J. A. Logan, C. A. Mims, G. W. Stewart and J. Ross, *J. Chem. Phys.*, 1976, **64**, 1804; (*b*) L. C. Brown, J. C. Whitehead and R. Grice, *Mol. Phys.*, 1976, **31**, 1069; (*c*) S. M. A. Hoffman, D. J. Smith, N. Bradshaw and R. Grice, *Mol. Phys.*, 1986, **57**, 1219.
2 F. E. Davidson, G. L. Duncan and R. Grice, *Mol. Phys.*, 1981, **44**, 1119.

Prof. R. Grice (*University of Manchester*) said: Does Mr Robinson conclude from the rebound distribution observed in his measurements on the CH_3+CF_3I exchange reaction that there is no significant well on the potential-energy surface corresponding to a stable $CH_3—I—CF_3$ radical intermediate?

Mr G. N. Robinson, Dr G. M. Nathanson, Mr R. E. Continetti and **Prof. Y. T. Lee** (*University of California, Berkeley, CA*) said: For polyatomic reactions, forward-backward symmetry in the product angular distribution and a product translational energy distribution that peaks near 0 kcal mol^{-1} are usually taken as evidence of a bound collision complex. From a study of the reaction $F+CH_3I \rightarrow IF\,CH_3$, Farrar and Lee[1] infer that $CH_3—I—F$ is bound by *ca.* 25 kcal mol^{-1} with respect to $F+CH_3I$. Likewise, reactive scattering studies of the reactions $CH_3+IY \rightarrow CH_3I+Y$[2*a*] and $Y+CH_3I \rightarrow IY+CH_3$[2*b*] (Y=Br, Cl) suggest that the $CH_3—I—Cl$ and $CH_3—I—Br$ intermediates are slightly bound. Thus it appears that one can correlate the I—Y attraction on a $CH_3—I—Y$ potential-energy surface with the electronegativity of the Y atom. The low electronegativity of the CF_3 group relative to the halogen atoms and the large repulsive energy release and strong backward scattering of the CH_3I product from the CH_3+CF_3I reaction suggest that $CH_3—I—CF_3$ is not bound by much energy, if at all.

1 J. M. Farrar and Y. T. Lee, *J. Chem. Phys.*, 1975, **63**, 3639.
2 (*a*) J. A. Logan, C. A. Mims, G. W. Stewart and J. Ross, *J. Chem. Phys.*, 1976, **64**, 1804; L. C. Brown, J. C. Whitehead and R. Grice, *Mol. Phys.*, 1976, **31**, 1069; S. M. A. Hoffman, D. J. Smith, N. Bradshaw and R. Grice, *Mol. Phys.*, 1986, **57**, 1219; (*b*) D. Krajnovich, Z. Zhang, F. Huisken, Y. R. Shen and Y. T. Lee, *Physics of Electronic and Atomic Collisions*, ed. S. Datz (North-Holland, Amsterdam, 1982), p. 733; S. M. A. Hoffman, D. J. Smith, A. Gonzalez Ureña, T. A. Steele and R. Grice, *Mol. Phys.*, 1984, **53**, 1067.

Prof. M. T. Bowers (*University of California, Santa Barbara, CA*) addressed Dr McKendrick. First, is the velocity distribution of the reactant $O(^3P)$ atoms known? What effect would significant changes in this velocity have on the reaction dynamics?

Secondly, have you considered calculating product rotational distributions using statistical methods simply by assuring rigorous conservation of the system angular momentum? This motion could well be decoupled from the clearly non-statistical product vibrational distribution.

Mr H. Rieley (*University of Bristol*) said: McKendrick *et al.* have presented the internal energy distribution for product OH from the simple chemical reaction $O(^3P)+HBr$. They were able to infer the opening of a reactive channel leading to production of the electronically excited partner $Br(^2P_{1/2})$ state, from an anomaly in the $OH(X\,^2\Pi, v''=1)$ rotational distribution. I would like to add to the list of novel diagnostics, given by Prof. Polanyi in his Spiers Memorial lecture, and demonstrate how velocity-aligned Doppler spectroscopy (VADS) could be a powerful tool in the determination of translational energy distributions of products from a bimolecular reaction (without the use of conventional time-of-flight techniques). Energy conservation may

then yield information about the distribution over energy states of a dark partner product, *e.g.* Br in the above reaction.

Wittig *et al.* have pioneered the VADS technique measuring the recoil velocity distribution of photofragment H atoms from various precursors.[1] By delaying the probe radiation following photolysis, fragments with velocity components perpendicular to the probe wave vector escape from the probe region and remain undetected. For a narrow velocity distribution the Doppler profile of the Lyman-α line of the H photofragment collapses to leave two outer wings, representing the speed along the probe direction. It is necessary to use suitably collimated beams and work at sufficiently low pressures to ensure a collision-free environment over the timescale of the experiment. A structured Doppler profile obtained under these conditions directly reflects the population distribution of the partner. This has been tested on the vibrational excitation of SH from photolysis of H_2S.[2] I wish to report here the first use of VADS on a species other than atomic hydrogen (namely OH), using laser-induced fluorescent (LIF) detection.

Presented in fig. 3 are some results obtained from a study of the photodissociation dynamics of nitrous acid (HONO) at 355 nm.[3] They show the evolution of a single OH(0, 0) line profile with increasing delay between pump and probe lasers. The change in Doppler profile is quite dramatic as the width of the angular distribution of recoiling OH sampled by the probe becomes smaller. No further significant narrowing of the profile was seen for $t > 800$ ns. Resolution is limited by both geometrical and molecular factors including, of course, the desired internal energy distribution of the partner NO fragment. In the work of Wittig and coworkers on photofragment H from HBr, the presence of both spin–orbit states of Br was resolved in the Lyman-α Doppler profile using a conventional dye laser with intracavity etalon.[2] In our own study, photofragment OH has recoil velocities an order of magnitude smaller than those of H, and the overall widths of the OH profiles are correspondingly narrower. As a result, it was necessary to improve the resolution of the probe radiation. This was achieved using a pulse-amplified c.w. dye laser system to give a linewidth of *ca.* 100 MHz in the u.v., providing a negligible contribution to the overall lineshape. The long delay profile reveals a narrow distribution in OH translation and indicates a narrow distribution in NO internal energy. It is possible to detect the NO fragment, also in LIF, and probe the internal distribution directly; and this has been done.

Fig. 4 shows rotational distributions obtained for NO($X\ ^2\Pi$, $v'' = 2$ and 3). They were obtained by reduction of representative branches from the one-photon LIF excitation spectra of the NO[($A\ ^2\Sigma^+$, $v' = 0$)–($X\ ^2\Pi$, $v'' = 2$ and 3)] bands. Tunable u.v. at the required wavelength was generated by Raman-shifting, in H_2, the doubled output of a Nd : YAG pumped dye laser. The distributions are approximately Gaussian in rotational quantum number, J: the $v'' = 2$ distribution peaks at *ca.* $J = 26$ with a half-width of *ca.* 15 and is the most highly populated, while that of $v'' = 3$ peaks at *ca.* $J = 21$ with a similar half-width. NO in $v'' = 1$ is partly obscured by photofragment NO from dissociation of NO_2 at 355 nm. However, population in levels higher than those allowed by the available energy for this latter process may be attributed to NO from photodissociation of HONO, and this shows a similar J-dependence, peaking around $J = 30$. Any nascent NO in $v'' = 0$ is completely obscured by a background of thermal NO. No population in $v'' = 4$ or 5 (the limit of available energy) was observed above the noise level. The main point to note is that each rotational distribution is narrow. As the peak value of J decreases with increasing vibrational quanta the distributions overlap significantly in total energy, resulting in a narrow distribution of internal energy overall. It is now possible to compare these two independent observations of NO internal energy.

Fig. 5 is an enlargement of the 1 μs delay spectrum from fig. 3, and marked along the Doppler shift axis are the positions corresponding to the total energies of the peaks in the NO($v'' = 2$ and 3) distributions. They agree favourably with the maxima in the observed OH translational energy distribution.

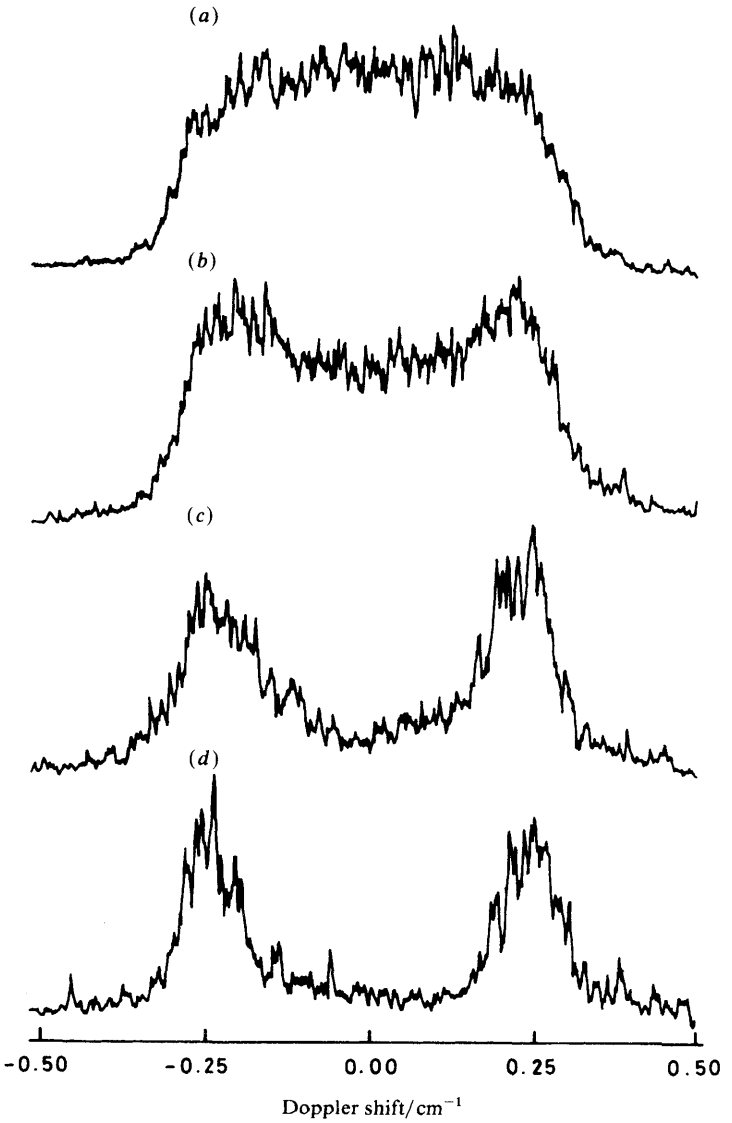

Fig. 3. Doppler profiles of the $P_1(2)$ line of OH[$(A\,^2\Sigma^+, v'=0)$-$(X\,^2\Pi, v''=0)$] at various delays between photolysis and probe. The delays are: (*a*) 0, (*b*) 200, (*c*) 600 and (*d*) 1000 ns, with photolysis at 355 nm.

In general, VADS should be a useful diagnostic method when there is a narrow internal energy distribution in a heavy recoiling partner. Consider probing the OH product from the reaction: $O(^3P)+HBr$. The partner Br is heavy (mass=80 a.m.u.) and has no internal degrees of freedom apart from the spin–orbit splitting energy of 3685 cm^{-1}. Therefore, at the threshold for production of the higher energy $^2P_{1/2}$ state, the difference in Doppler shifts for a line in the OH(1, 1) band will be *ca.* 0.24 cm^{-1}. This may be resolvable even with a conventional dye-laser system. In photodissociation, the loss of resolution in a Doppler profile from VADS is partly due to the internal energy distribution in the recoiling partner, the thermal motion of the parent, and the finite size and profile

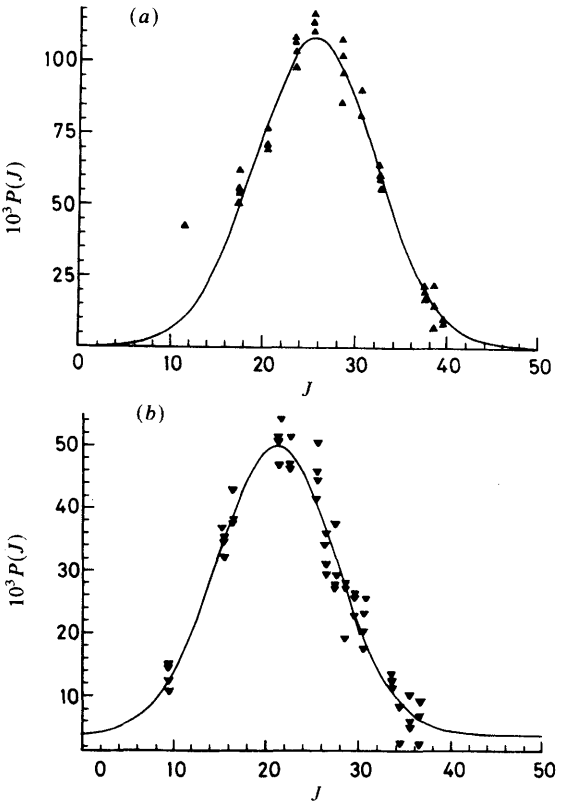

Fig. 4. Nascent NO rotational distributions, $P(J)$, from the photodissocation:

$$HONO(v_2 = 2) \xrightarrow{355\ nm} OH(X\ ^2\Pi) + NO(X\ ^2\Pi, v'').$$

(*a*) $v'' = 2$, $R_{22}(J)$. (*b*) $v'' = 3$, $Q_{21}/R_{11}(J)$.

of the laser beams. For a chemical reaction there may be further averaging due to a spread of reactive collision energies. The latter is the main source of complication for the reaction under discussion as the collision energy depends on the internal energy distribution of NO from the photodissociation of NO_2, the precursor of $O(^3P)$. However, the energy available from this process is *ca.* 3000 cm^{-1}, and the range of reactive collision energies should not obscure the partner product distribution completely. It should therefore be possible to distinguish the spin-orbit states of product Br in the translational energy spectrum of OH and, perhaps more interestingly, correlate the Br spin-orbit branching ratio with OH internal energy states by performing VADS on different transitions.

The feasibility of applying VADS to molecular products from a chemical reaction has been demonstrated. It is easy to envisage a number of simple chemical systems for which VADS could be used to determine cross-correlations between the quantum states of two molecular products. Indeed, a significant improvement may be gained over the experiment described above, by using a collimated molecular beam source, crossed at right-angles by the laser beams, to minimise any parallel velocity component from parent molecules, thereby further improving the energy resolution.

1 Z. Xu, B. Koplitz, S. Buelow, D. Baugh and C. Wittig, *Chem. Phys. Lett.*, 1986, **127**, 534.
2 Z. Xu, B. Koplitz and C. Wittig, *J. Chem. Phys.*, 1987, **87**, 1062.
3 H. Rieley, *PhD Thesis* (University of Bristol, 1988).

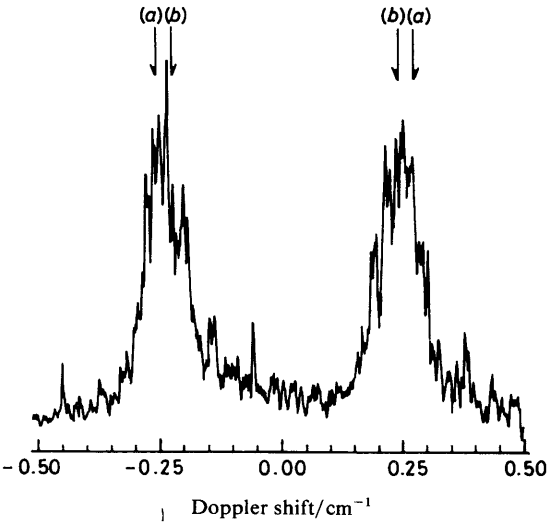

Fig. 5. An enlargement of the 1 μs delay Doppler profile of the $P_1(2)$ transition: (a) and (b) are the Doppler shifts which, by energy conservation, correspond to the peaks in the rotational distributions of NO, $v''=2$ and 3, respectively.

Prof. S. R. Leone (*University of Colorado, CO*) said: There are many different mechanisms that can lead to bimodal rotational distributions. We have seen several of these, and it is useful to formulate a more complete list. Different rotational distributions can be the result of different macroscopic product branches, such as suggested in the paper by Zare for the Br($^2P_{1/2}$) and Br($^2P_{3/2}$) states in the O+HBr reaction. Also possible are the direct *versus* migratory pathways (microscopic branches) referred to in the paper by Grice. We have learned many details of bimodal rotational distributions in the photofragmentation of bent *versus* linear states. In addition, it is important to consider the possibility that different rotational sub-branches could result from various spin–orbit states in the reagents. For example, the O($^3P_{2,1,0}$) states in O+HBr could lead to spin–orbit-selective reactivity and selective rotational population groups. In atoms such as O($^3P_2$), the possibility also exists for orbital alignment effects, which may connect to specific rotation states. It has already been pointed out in the paper by Zare that the final OH spin–orbit states may be connected in a selective manner to the O($^3P_{2,1,0}$) reagent states. Tunnelling effects might also lead to different rotational states. Finally, in ion–molecule systems, potential surface hopping on the inward or outward parts of the trajectories may result in different rotational states from the varying topologies in the exit part of the trajectory.

Prof. L. Holmlid and **Dr P. A. Elofson** (*University of Göteborg, Sweden*) said: We wish to comment on the experiments on O(^3P)+HBr by McKendrick, Rakestraw and Zare. We have applied our statistical simulation algorithm to the calculation of the vibrational energy distributions for this reaction, using the experimental conditions in our calculations. The procedure we use simulates the reaction for each of a large number of colliding, reacting molecules and distributes the energy in a unimolecular (RRKM) fashion over the pertinent energy terms ('boxes'). In this case, four boxes were used: molecular vibration and rotation, orbital motion and relative translation. Angular momentum and reactive flux are conserved strictly. Angular-momentum conservation restricts the number of available configurations at the transition states (centrifugal barriers) severely. In the present calculation, quantization of vibrational energy is

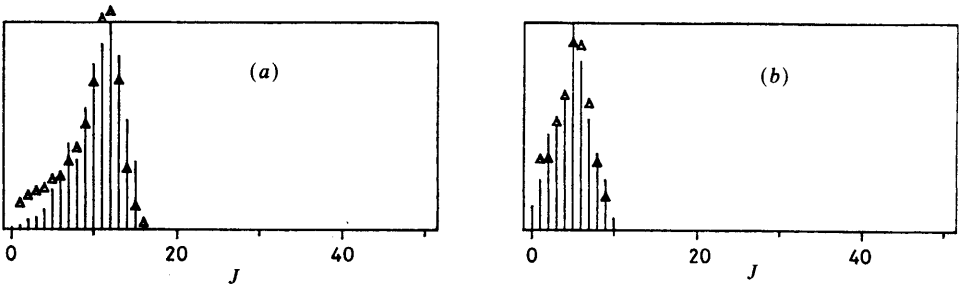

Fig. 6. Distributions of rotational quantum number J for $v'=1$ (a) and 2 (b). Triangles are experimental results from McKendrick *et al.*

included also in the product channel, *i.e.* for OH in the form of a 'window' technique. In this way only simulated systems with vibrational energies within small limits around each vibrational energy level (*ca.* 1% of $\hbar\omega$) are allowed to move into product space. Systems that fail to meet this criterion go through a new energy distribution calculation. In this way, all complexes are forced into small energy bands around the quantum-mechanically allowed vibrational levels.

Our result for the rotational J distributions, in fig. 6, match the experiments very well. At low J_{rot} and $v'=1$, the discrepancy is probably due to Br* formation as concluded by Prof. Zare's group. Rotational distributions of this type have been found for other systems as well. Our previous calculations[1,2] on systems like $O(^1D)+H_2$, HCl show good agreement with experiments also in this respect. The rotational inversion is due to the angular-momentum restrictions, as shown by our results using this purely statistical theoretical description.

In the case of vibrational energy descriptions, we can match the experiments by arbitrarily introducing a variation of the 'window' width with quantum number. Without such a procedure our calculations still give a large number of systems in $v'=0$, as seen in fig. 7. We propose that the 'window' size variation is due to differences in the coupling of the orbital and rotational angular momenta at the transition state. For small v', rotational energy is large, and the angular momenta are almost at right angles to each other, thus giving a small anisotropy of the potential between Br and OH and a small broadening of the OH vibrational levels. For large v', the angular momenta become more parallel, the anisotropy in the Br—OH interaction increases and so does the broadening of the OH vibrational levels.

We would like to conclude about this reaction as follows: (1) rotational distributions are statistical, even if they are inverted; (2) vibrational distributions may be statistical when the vibrational level 'broadening' proposed above is included; (3) even short-lived complexes like OHBr may decompose statistically.

1 P. A. Elofson, K. Rynefors and L. Holmlid, *Chem. Phys.*, 1985, **100**, 39.
2 K. Rynefors, P. A. Elofson and L. Holmlid, *Chem. Phys.*, 1985, **100**, 53.

Prof. D. W. Setser (*Kansas State University, KS*) said: Zare and coworkers have measured the vibrational and rotational distribution for OH from the $O(^3P)+HBr$ reaction. They discuss the results in terms of the kinematic constraints imposed by the **H+LH** mass combination. They also suggest that the rather high rotational distribution found for OH(v=1 and 2) could be associated with repulsive energy release from a bent O—H—Br configuration in the exit channel. We have utilized exoergic H abstraction reaction by $O(^3P)$ atoms to investigate[1] the **H+LH** kinematic constraints

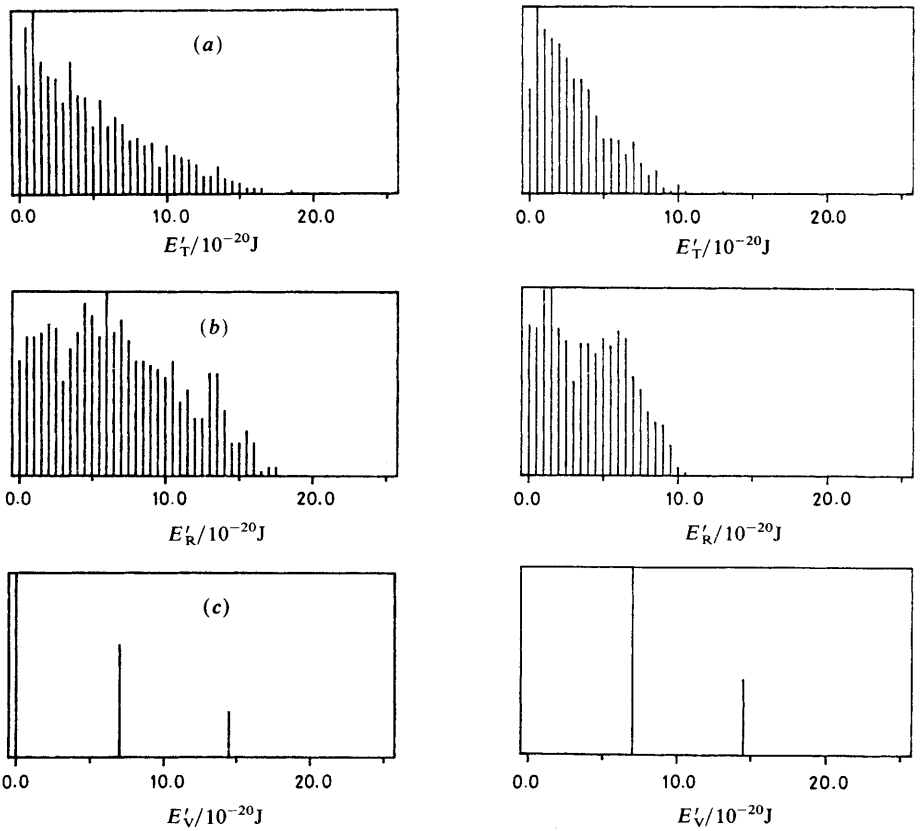

Fig. 7. Energy distributions for the OH products, [(*a*) translational, (*b*) rotational and (*c*) vibrational] using a vibrational level width of 0.5% of $\hbar\omega$ to the left. To the right, the level width has been varied to reach approximate agreement with experiments. Rotational J distributions for $v'=1$ and 2 are unchanged during this process.

to vibrational energy disposal; the results can be compared to F atom reactions for HI, GeH_4, SiH_4 and SeH_2 as reagents.[2,3]

Our experiments[1] were done in a fast flow reactor in which the product vibrational states were observed after *ca.* 0.2 ms of reaction time. The O atoms were produced by microwave discharge in Ar. Laser-induced fluorescence was used to measure the ratio of the OH($v=0$) to OH($v=1$) concentration, and infrared chemiluminescence was used to measure the relative populations of OH($v=1$, 2 and 3). The vibrational distributions are summarized in table 1, and $\langle f_V(OH)\rangle$ is compared with $\langle f_V(HF)\rangle$. No information was obtained about rotational, spin-orbit or λ-doublet populations of OH, since these levels exhibited Boltzmann distributions for our operating conditions of 0.5 Torr and 300 K.

All OH vibrational distributions are inverted, with the OH(v, J) populations extending to the thermochemical limits. The vibrational energy disposal to OH(v) is very similar to that for HF(v) from F-atom reactions, even to the extent of having the same linear surprisal plots.[3] This is true in spite of the much smaller (two orders of magnitude)

Table 1. Vibrational energy disposal summary

reaction	$\langle E \rangle$ /kcal mol^{-1}	P_0	P_1	P_2	P_3	$\langle f_V(OH) \rangle$	$\langle f_V(HF) \rangle$
O+HI	35.4	13	11	34	42	0.56	0.59
O+GeH_4	28.4	18	31	47	03	0.47	0.59
O+SiH_4	17.0	19	81			0.49	0.52
O+SeH_2	30.3	24	36	40		0.38	0.48

rate constants for the O-atom reactions. Thus the kinematic constraints to vibrational energy disposal imposed upon direct H abstraction by O(^3P) atoms is confirmed. We agree with Zare and co-workers in that the O(^3P) reactions with H-containing molecules show no indication of a component proceeding *via* non-adiabatic pathways to a lower-energy singlet surface corresponding to bound singlet molecules.

We interpreted the rather high OH(v=0)/OH(v=1) ratio from O+HI as possibly being the consequence of I($^2P_{1/2}$) formation.[1] If the higher-energy spin-orbit state is formed, energy constraints limit the OH product to $v \leq 1$. The mechanism for I($^2P_{1/2}$) formation could be V-E energy transfer in the exit channel, as advocated for Br($^2P_{1/2}$) formation in the F+HBr reaction.[4,5] In our work the ratio OH(v=0)/OH(v=1) was measured as a function of added reagent, and the ratio was invariant. Nevertheless, residual OH(v=0) emanating from the microwave discharge source of O atoms would make the measured ratio an upper limit to the true ratio from the chemical reaction.

The rotational energy disposal from F atom reactions[6,7] with HCl, HBr and HI can be examined for insight with respect to the O+HBr reaction. Each HF(v) level tends to have approximately the statistically expected mean rotational energy when examined in terms of the reduced variable $g_R = f_R/(1-f_V)$, and the overall $\langle g_R(HF) \rangle$ are 0.3–0.4.[6,7] Quasi-classical trajectory calculations for LEPS type surface having the lowest barrier for collinear geometry give qualitatively similar rotational energy disposal.[7] For the polyatomic hydride molecules, $\langle f_R(HF) \rangle$ seems to increase as the reaction cross-section becomes larger, until the limit just mentioned for the diatomic molecules is reached.[3] Thus I would like to propose a question to Prof. Herschbach and Zare (and others) with respect to kinematic constraints to the rotational energy disposal for the **H+LH** mass combination. Will reduced reactive cross-sections (with increased barrier heights) make significant changes in the expected kinematic constraints to rotational energy disposal? Stated in more specific terms, is a bent configuration in the exit channel required to explain the rotational energy release for the O+HBr reaction *vis-à-vis* comparison to the F-atom reactions, which presumably proceed *via* collinear geometry?

1 B. S. Agrawalla and D. W. Setser, *J. Chem. Phys.*, 1987, **86**, 5421.
2 B. S. Agrawalla and D. W. Setser, *J. Phys. Chem.*, 1986, **90**, 2450.
3 B. S. Agrawalla and D. W. Setser, in *Gas-phase Chemiluminescence and Chemi-ionization*, ed. A. Fontijn (Elsevier, Amsterdam, 1985).
4 J. P. Sung and D. W. Setser, *Chem. Phys. Lett.*, 1977, **48**, 413.
5 J. W. Hepburn, K. Liu, R. G. Macdonald, F. J. Northrup and J. C. Polanyi, *J. Chem. Phys.*, 1981, **75**, 3353.
6 K. Tamajake, D. W. Setser and J. P. Sung, *J. Chem. Phys.*, 1980, **73**, 2203.
7 P. Beadle, M. R. Dunn, N. B. H. Jonathan, J. P. Liddy and J. C. Naylor. *J. Chem. Soc., Faraday Trans. 2*, 1978, **74**, 2170.

Prof. D. R. Herschbach (*Harvard University, MA*) (*communicated*): Prof. Setser invited comment on kinematic constraints for the rotational energy disposal in reactions having the heavy + light-heavy mass combination, such as O+HBr. In particular, he asked (1) whether reduced reaction cross-sections resulting from high barriers might significantly alter the constraints and (2) whether a bent configuration in the exit valley

is required to account for the high product rotational excitation found for O + HBr. He noted that this high excitation resembles that for F + HBr, which is presumed to react collinearly. I think the answer to (1) is *yes*. For instance, a high barrier might confine reaction to small impact parameters and thereby weaken the propensity for approximately equal reactant and product orbital angular momenta.

I think the answer to (2) is *no* in principle but quite likely *yes* in practice. The 'in principle' aspect is akin to the situation described in our paper, in which high product rotational excitation is fostered by antiparallel alignment of orbital and rotational momenta. For instance, suppose $\boldsymbol{j}$ can be neglected and an entrance barrier renders the typical $\boldsymbol{l}$ unusually small. Then even when the reaction involves no change in reduced mass, a large exit velocity or impact parameter can make the typical $\boldsymbol{l}'$ substantially larger than $\boldsymbol{l}$ and thus yield high product rotation, $\boldsymbol{j}' = \boldsymbol{l} - \boldsymbol{l}'$.

The 'in practice' aspect is exemplified in several studies cited by McKendrick, Rakestraw and Zare and by Amaee, Connor, Whitehead, Jakubetz and Schatz in their papers. Also especially pertinent are recent trajectory calculations by Persky and Kornweitz.[1] They compare results obtained for the Cl + HCl reaction with three semi-empirical LEPS potential-energy surfaces, designated I–III. For each, the preferred reaction configuration is collinear. The activation barrier is large; its height is the same for the collinear configuration (8.55 kcal mol^{-1}) but increases more steeply for bent configurations as surface I → II → III. Despite this, the reactive cone of acceptance increases considerably in the same order. That happens because surfaces II and particularly III exert strong anisotropic attractive torques which pull the reactant molecule into a nearly collinear orientation even when the initial approach angle is unfavourable. As in previous studies, the product rotational excitation reflects repulsive torques in the exit valley. For surface III a nearly collinear configuration usually persists well into the exit trajectory, and the products emerge with only low rotational excitation. For surface I, although the critical reactive configurations are likewise nearly collinear, strongly bent configurations are attained early in typical exit trajectories. In these bent configurations, repulsion sets the light hydrogen atom spinning and produces high rotational excitation.

Collinear reaction in the entrance valley and saddle-point regions is a property distinct from repulsive torques in the exit valley. Until we can reliably derive these forces from electronic structure, our diagnostic criteria remain provisional. However, in view of the special kinematics for heavy + light–heavy systems and the extensive trajectory studies, high product rotational excitation offers strong evidence that repulsion occurs in bent configurations early in the exit valley. This seems likely for the reactions of both F atoms and O atoms with hydrogen halides.

1 A. Persky and H. Kornweitz, *J. Phys. Chem.*, 1987, **91**, 5496.

Dr E. J. Kruus, Dr B. I. Niefer and **Dr J. J. Sloan** (*NRC, Ottawa, Canada*) said: We have measured the product state distributions from the corresponding reactions of $O(^1D)$ with HCl and HBr, using a novel implementation of time-resolved Fourier transform spectroscopy (TRFTS) to observe the infrared emission spectra of the products. $O(^1D)$ atoms were created by pulsed laser photolysis of ozone. The experiments were carried out at total reagent pressures (ozone and HCl or HBr) of a few mTorr. The submicrosecond time-resolution of the TRFTS technique permits the product emission spectra to be observed at approximately each gas-kinetic collision after the $O(^1D)$ atom is created. In this way, both the unrelaxed (initial) product energy distributions and the energy transfer pattern resulting from the collisional deactivation of the vibrationally excited product can be observed.

Emission spectra from both OH and HCl created by the reaction, recorded at *ca.* 2, 10 and 30 gas-kinetic collisions after the ozone photolysis, are shown in fig. 8. From the measured spectral intensities and the known Einstein transition probabilities, the

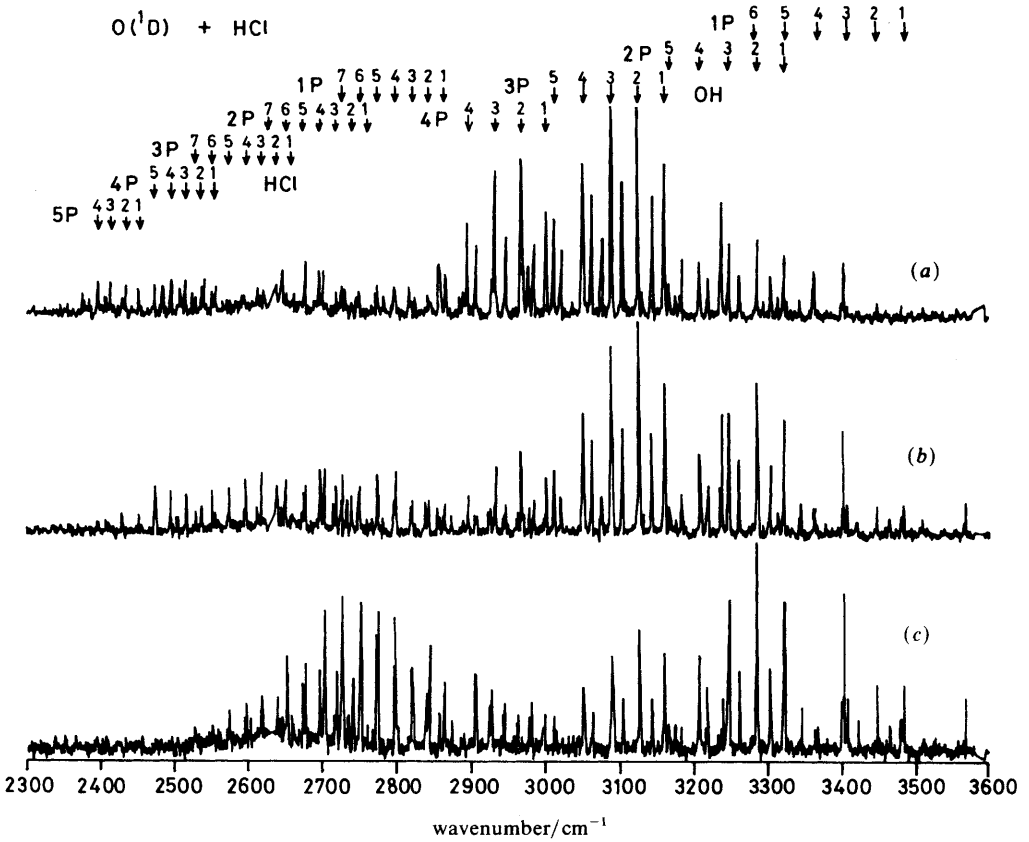

Fig. 8. Infrared emission spectra from the unrelaxed OH(v') and HCl(v') products of the reaction: O(^1D) + HCl, recorded using fast time-resolved Fourier transform spectroscopy. τ_D = (*a*) 20, (*b*) 100 and (*c*) 300 μs.

ratio of the cross-section for reaction: O(^1D) + HCl → OH(v') + Cl to that for E-V energy transfer producing O(^3P) + HCl(v'), is found to be 0.95–0.05. The initial vibrational distributions in both channels are strongly inverted; but they relax rapidly in subsequent collisions. Fig. 9 (*a*) and (*b*) show, respectively, the time dependences of the OH(v') and HCl(v') distributions. Details of these will be presented elsewhere.[1] The reaction and the E-V energy transfer process channel 64 and 62%, respectively, of the reaction exoergicity into product vibration. Very similar results were obtained for the O(^1D) + HBr reaction, which creates both OH and HBr with strong vibrational inversion as well.

The singlet reactions occur on electronic surfaces which are topologically quite different from those of the triplet reactions. The O(^3P)/HX (X=Cl or Br) surfaces are monotonically exothermic, having no minima; whereas the singlet surfaces for both reactions studied in our work correlate with strongly bound intermediates of the form H—O—X. As reported in the study of McKendrick *et al.*, the triplet reactions are probably simple hydrogen abstractions, having the expected dynamics for the heavy-light-heavy mass combination in direct reactions. If the singlet reactions are insertions, accessing the strongly bound intermediate, the strong inversions observed must be due to dynamical constraints limiting the energy randomization which would be expected to occur during the lifetime of the intermediate. Similar effects have been seen in the

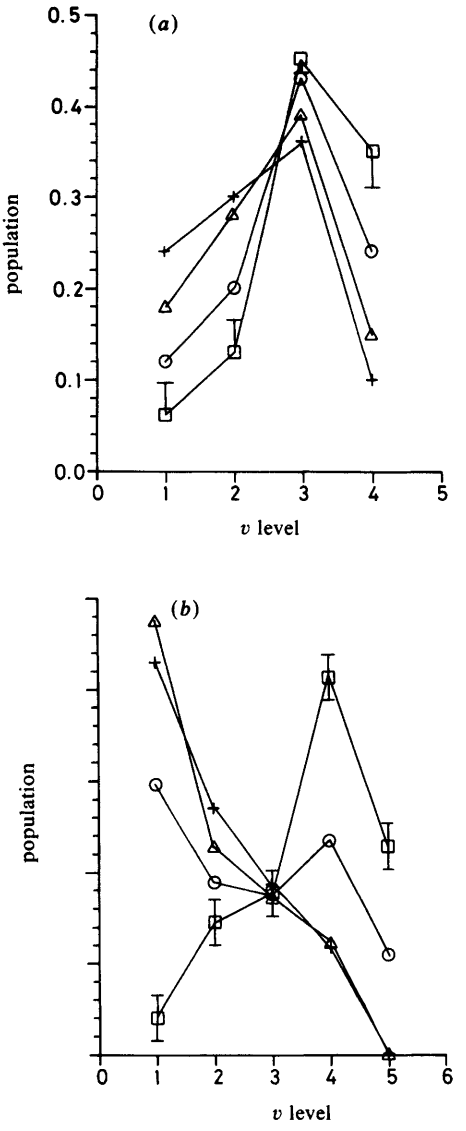

Fig. 9. The time dependences of (a) the OH(v') vibrational distribution created in the reaction: $O(^1D)+HCl \rightarrow OH(v')+Cl$; and ($b$) the HCl created in the E-V energy transfer: $O(^1D)+HCl \rightarrow HCl(v')+O(^3P)$. $\langle Z_{GK} \rangle$ is the average number of gas-kinetic collisions suffered by the product molecules at the time of observation: □, 4; ○, 6; △, 13 and +, 18.

case of the $O(1D)/H_2$ reaction, for which it has been shown[2,3] that the lifetime of the analogous H—O—H intermediate is too short to permit energy randomization.

1 E. J. Kruus, B. I. Niefer and J. J. Sloan, *J. Chem. Phys.*, 1988, in press.
2 P. M. Aker and J. J. Sloan, *J. Chem. Phys.*, 1986, **85**, 1412.
3 P. J. Kuntz, B. I. Niefer and J. J. Sloan, *J. Chem. Phys.*, 1988, in press.

Prof. D. G. Truhlar (*University of Minnesota, MN*) said: Based on earlier theoretical studies employing classical trajectories, McKendrick, Rakestraw and Zare present an interesting interpretation of the inverted product vibrational distribution for the reaction

O + HBr → OH + Br in terms of trajectories in which the H atom is transferred at relatively large internuclear distances. Another possibility is evident from our earlier semiclassical calculations on the similar exothermic reaction Cl + HBr → ClH + Br on a model potential-energy surface.[1] In that study we found that reaction under room-temperature thermal conditions was dominated by tunnelling, and the product population inversion arose naturally as a consequence of shorter tunnelling paths in the mass-scaled coordinate system for tunnelling into vibrationally excited product channels. Since the O + HBr → OH + Br reaction has a significant classical barrier, and since hydrogen-atom transfer reactions involving a significant barrier are usually dominated by tunnelling,[2] I would suggest that this vibrationally assisted tunnelling mechanism probably controls the dynamics under room-temperature thermal conditions, and further interpretation of the details of the product distribution should include this mechanism, at least under such low-energy conditions.

1 B. C. Garrett, N. Abusalbi, D. J. Kouri and D. G. Truhlar, *J. Chem. Phys.*, 1985, **83**, 2252.
2 R. T. Skodje, D. G. Truhlar, and B. C. Garrett, *J. Phys. Chem.*, 1982, **77**, 5955; D. G. Truhlar and B. C. Garrett, *Annu. Rev. Phys. Chem.*, 1984, **35**, 159; *J. Chim. Phys.*, 1987, **84**, 365.

Dr K. G. McKendrick (*Stanford University, CA*) replied: Prof. Bowers has inquired about the O(^3P) atom velocity spread following the 355 nm photolysis of NO_2, and the effect that this might have on our observations. As briefly discussed in our paper, two previous studies have been reported of energy deposition in the fragments of NO_2 photolysed at wavelengths close to 355 nm [347 and 337 nm; ref. (40) and (41) of our paper, respectively]. These studies, although not directly comparable given the slightly different wavelengths, are in contradiction over the partitioning of available energy between translational and internal degrees of freedom. {The time-of-flight measurements [ref. (40)] imply a greater proportion of energy appearing as fragment translation than measurements [ref. (41)] of the internal state populations of NO.} Although no equivalent measurements have been reported for photolysis at 355 nm, it is clear that in our experiment there will be a relatively broad distribution of O(^3P) velocities and hence O + HBr collision energies, extending to the approximate energetic limit (*ca.* 25 kJ mol^{-1}) derived in our paper.

We also discuss in our paper some general aspects of the dynamics of reactions with the heavy + light-heavy (H + LH′) mass combination, the kinematic category to which O + HBr belongs. A number of generalisations have been derived from several independent studies. The propensity [expressed in eqn (4) of our paper] for translational energy to be approximately conserved during the reaction, which was reproduced in our quasi-classical trajectory (QCT) calculations on the O + HBr system using the LEPS surface derived by Persky and coworkers, implies that a distribution of collision energies will have a relatively minor effect on the measured product internal state distributions. For example, in our QCT calculations, we find that on increasing the collision energy from 15 to 25 kJ mol^{-1} (corresponding to the range from slightly above the classical dynamical threshold to the limiting collision energy in our experiment) the average internal energy of the products increases by only 1.3 kJ mol^{-1}. We therefore feel that the interpretation of our results is not seriously complicated by the distribution of O(^3P) velocities resulting from their method of production.

Mr Rieley has suggested an indirect method for the estimation of the branching ratio Br*/Br [*i.e.* Br($^2P_{1/2}$)/Br($^2P_{3/2}$)] from the reaction O(^3P) + HBr. It is, of course, possible to measure this quantity directly by spectroscopic means, *e.g.* by laser gain/absorption, multiphoton ionisation, or v.u.v. fluorescence. Using the last of these techniques, Polanyi and coworkers[1] have determined the Br*/Br ratio from the closely related reaction F + HBr → FH + Br, finding *ca.* 6% branching into the spin-orbit excited state.

As discussed in our paper, we have associated the low N'' inflection in the reduced OH($v''=1$) rotational distribution with the channel leading to Br*. For the purposes

of estimating this branching ratio, we may assume that the shape of the rotational surprisal plot associated with a single channel is the approximately parabolic function obtained in a previous study of a similar H + LH′ system, Cl + HCl (to be discussed later in this meeting[2]). A similar dependence was also found in our QCT calculations on O + HBr, and is consistent with the propensity rule (4) of our paper which predicts that the product state distribution is expected to peak sharply at an energy approximately isoenergetic with the reagents. The difference between the actual experimental surprisal and the extrapolated (postulated) parabolic plot corresponds to *ca.* 6% 'extra' population in the low N'' states of OH($v''=1$). This value is interestingly similar to the 6% Br* branching in the F + HBr system.[1]

Prof. Leone has remarked on the different processes which can give rise to multimodal product state distributions, and in particular has raised the question of the role of the O(^3P_J) reagent fine-structure state distribution in determining the product-state fine-structure partitioning.

An argument of partial electronic adiabaticity has previously been presented by Andresen and Luntz [ref. (13) of our paper] as an interpretation of the OH fine-structure state partitioning in the products of O(^3P) reactions with organic molecules. However, by variation of the F*/F ratio in the F atom source, Polanyi and coworkers[1] were able to demonstrate that the Br*/Br ratio was not determined by the reagent fine-structure state distribution in the F + HBr system. It was argued that the Br* branching was controlled by non-adiabatic coupling between surfaces in the exit channel region.

In a similar fashion, we have performed a second series of investigations of the O + HBr system using microwave discharge of molecular O_2 as an alternative method for O(^3P) generation. An effusive jet of O(^3P) was crossed by a pulsed supersonic free jet of HBr seeded in a carrier gas (generally He). The O(^3P_J) fine-structure state distribution in the case of microwave discharge generation will be that of a thermalised sample (as a result of many downstream gas-phase and wall collisions). Unfortunately, the O(^3P_J) distribution following 355 nm photolysis of NO_2 is unknown. However, it would be highly coincidental if the distributions from the two methods of production were to be identical. Nevertheless, we observe that the OH $^2\Pi_{1/2}/^2\Pi_{3/2}$ ratio is the same, within experimental error, in the complementary measurements. It seems therefore most likely that this aspect of the product-state partitioning is not determined by the reagent-state distributions.

Similarly, it would be interesting to assess any dependence of the Br*/Br ratio on the method of O-atom production. However, we were experimentally prevented from making this determination because, in the effusive beam/supersonic jet experiments, the low rotational state populations of OH were perturbed by a contribution from reaction with HBr van der Waals clusters formed in the free-jet expansion.[3] (Recall that we are presently only postulating the occurrence of Br* production by an indirect analysis of the OH rotational distribution.) An interesting extension to our work would clearly be to examine in more detail the dependence of the product fine-structure state partitioning on controlled reagent fine-structure populations.

I turn now to Prof. Holmlid, Bowers and Setser.

There have been several comments concerning the relationship of our experimentally observed product state distributions to those expected from statistical considerations. We have not considered that a statistical approach to the interpretation of the data would be the most fruitful, primarily because of the very heavily inverted OH vibrational distribution (which is contrary to the concepts of statistical energy partitioning). Therefore, we have approached the problem from a dynamical standpoint, implicitly assuming that the product state attributes are deterministically related to the properties of the potential-energy surface describing the three-body interaction. The quasi-classical trajectory calculations which we have performed on the potential surface derived by Persky and coworkers, with initial conditions selected in the usual Monte Carlo fashion from

Table 2. Calculated and measured moments of the distributions

	$\langle f_{vib} \rangle$	$\langle f_{rot} \rangle$	$\langle f_{trans} \rangle$
exptl	0.51	0.24	(0.25)
QCT	0.52	0.22	0.26

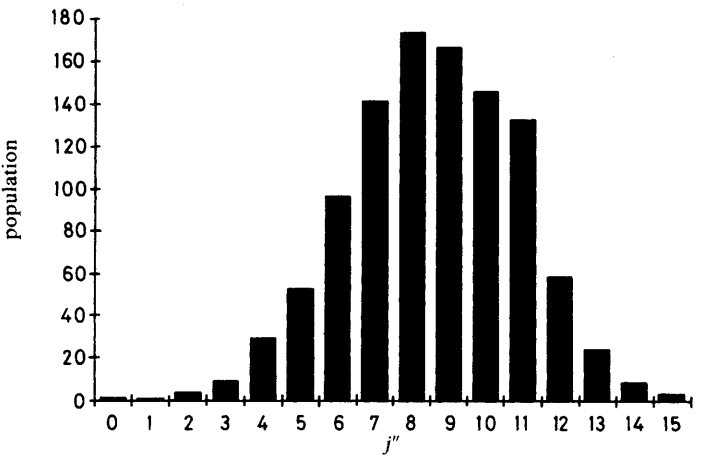

Fig. 10. Rotational distribution in OH($v''=1$) predicted by quasi-classical trajectory calculations on the reaction O(^3P)+HBr, assuming a uniform collision energy distribution over the range 15–25 kJ mol^{-1}.

distributions designed to simulate our experiment, have yielded results in very satisfactory agreement with the experimental observations. The calculated moments of the distributions are particularly close to the measured values, as shown in table 2.

The detailed distributions are in good qualitative but not perfect quantitative agreement: this is perhaps unsurprising for the vibrational distribution, where the quasi-classical '*post hoc*' quantisation of the distribution is highly arbitrary, given that the product energy space spans only *ca.* two vibrational quanta. Although the QCT calculations correctly predict the heavy vibrational inversion of OH($v''=1$) over OH($v''=0$), they fail to reproduce the experimentally observed 10% branching into $v''=2$. The calculated OH($v''=1$) rotational distribution (treating OH as a $^1\Sigma$ molecule) correctly shows a peak at relatively high j'', but at 1 or 2 quanta below that of the experimental distribution, as shown in fig. 10 (*cf.* fig. 3 of our paper).

We therefore feel that a dynamical interpretation provides a satisfactory rationalisation of both rotational and vibrational product attributes. It is interesting that Prof. Holmlid's calculations, using a statistical algorithm which incorporates rigorously the conservation of total angular momentum, reproduce well the OH rotational distributions from the O+HBr reaction. Perhaps this is indicative that this aspect of the product state partitioning (in this particular case) is controlled primarily by kinematic rather than authentic dynamical influences. Setser has further commented on the similarity between the H atom abstraction reactions of F and O atoms with certain reagents, and questions the role of repulsive energy release in determining the product state distributions in these systems. One might also consider related systems which share common kinematics, but which exhibit dramatically contrasting dynamics, *e.g.* the respective

rotationally 'hot' and 'cold' OH distributions formed in the reactions of $O(^3P)$ with HBr and organic molecules. These differences can be rationalised in a dynamical picture[3] in terms of the constraint towards collinearity in the controlling potential surface, which markedly affects the degree of rotational excitation of the products.

Is a statistical model capable of reproducing such contrasting behaviour? More generally, what physical interpretation should be attached to the ability of statistical modelling to rationalise partially the observed product state attributes (rotational but not vibrational distributions)?

Finally I reply to Dr Sloan and Prof. Truhlar. Dr Sloan has presented experimental results for the reactions of electronically excited $O(^1D)$ with HBr (and HCl), and has remarked on the qualitative similarity of the product state energy partitioning in the reactions of $O(^3P)$ and $O(^1D)$ with HX molecules. As he points out, the $O(^1D)$ reactions are considered to proceed on the ground-state singlet surface *via* transitory insertion of the O atom into the HX bond. Reaction is still direct, however, in the sense that the HOX intermediate survives for a time much shorter than that required for energy randomisation to take place and for corresponding 'statistical' (a term perhaps to be used rather cautiously) product state distributions to result. Whilst we are able to reproduce our observations by performing trajectory calculations on a surface which restricts reaction to direct abstraction, it is well known that it is not possible uniquely to invert product state distributions to recover the form of the potential surface. We are therefore not able to exclude rigorously the possibility that the $O(^3P)$ + HBr reaction alternatively proceeds *via* O-atom insertion into the HBr bond, involving a non-adiabatic curve-crossing from the initial triplet surface.

Insight into alternative mechanisms for these reactions would certainly be aided by the calculation of realistic *ab initio* potential-energy surfaces (ideally of both multiplicities and for all fine structure states), a development which we would like to encourage strongly.

Prof. Truhlar has commented on a possible role for tunnelling in this light-atom transfer reaction. Under the slightly superthermal conditions of our experiment, a significant proportion of collisions occur at energies above the classical barrier height, tending to reduce the importance of the contribution to reaction from tunnelling. More generally, the barrier height on a potential-energy surface derived from the comparison of classical calculations with experiment will be correspondingly underestimated to compensate for the extent to which tunnelling is important. It would be interesting to determine whether significant differences are predicted between the product state distributions of a more rigorous calculation, including the effects of tunnelling, and those of a quasi-classical calculation with an artificially reduced barrier height.

1 J. W. Hepburn, K. Liu, R. G. Macdonald, F. J. Northrup and J. C. Polanyi, *J. Chem. Phys.*, 1981, **75**, 3353.
2 B. Amaee, J. N. L. Connor, J. C. Whitehead, W. Jakubetz and G. C. Schatz, *Farday Discuss. Chem. Soc.*,1987 **84**, 387.
3 Full details of further experimental investigations and QCT calculations will appear in a forthcoming paper: K. G. McKendrick, D. J. Rakestraw and R. N. Zare, *J. Phys. Chem.*, in press.

Prof. P. J. Dagdigian (*The Johns Hopkins University, Baltimore, MD*) and **Prof. M. H. Alexander** (*University of Maryland, MD*) said: There has been considerable confusion in the past about the symmetry properties of Λ doublet levels in Π electronic states. Preferential population of Λ doublet components in collision phenomena can provide incisive information on the dynamics of these processes. Several years ago we[1] presented a detailed exposition of the reflection symmetry of the electronic wavefunction for molecules in Π electronic states, concentrating in particular on $^1\Pi$ and $^2\Pi$ states. We showed the relationship between the total parity, *i.e.* the *e* and *f* labels, the spectroscopic branch employed and the reflection symmetry of the Λ doublet level probed. More recently we have extended this analysis in detail for $^3\Pi$ electronic states.[2]

For one of the Λ doublet levels, the electronic wavefunction is symmetric with respect to reflection of the spatial coordinates in the plane of rotation in the high-J limit, while for the other it is antisymmetric. The analysis of the reflection symmetry of only the spatial coordinates of the electrons implies that the same measure of electronic asymmetry can be applied to wavefunctions in both the Hund's case (a) limit, where the spin is coupled to the molecule-frame z-axis, and in the case (b) limit, where the spin is coupled to the space-frame Z-axis. This type of analysis is particularly appropriate to interpretations of reactions and photodissociation processes in which arguments based on the evolution in space of the molecular orbitals of the precursor species are used to interpret the preferential production of a given Λ-doublet. At present, however, there is no convenient and unambiguous way to designate concisely these symmetry properties. In the literature, the two Λ doublet levels of a Π electronic state are often designated by Π^+ and Π^-, but the meaning of these labels is not consistent in all papers. In their contribution to this Discussion, McKendrick, Rakestraw and Zare have proposed a new notation, $\pi(\|J)$ and $\pi(\perp J)$, which describes the orientation of the unpaired $p\pi$ electron lobe with respect to the angular momentum vector $\boldsymbol{J}$. In the former type of level, the $p\pi$ lobe is parallel to $\boldsymbol{J}$, and hence perpendicular to the plane of rotation in the high J limit, while for the latter, the $p\pi$ lobe is in the plane of rotation.

Subsequent to the writing of the paper of McKendrick *et al.*, we have had discussions with Prof. Zare on this question of the notation of Λ doublet levels and have agreed upon a notation which we believe is more descriptive for use by scattering-dynamicists. We propose the alternative notation $\Pi(A')$ and $\Pi(A'')$. The label $\Pi(A')$ designates Λ doublet levels whose electronic coordinates are symmetric with respect to reflection of the electronic spatial coordinates in the plane of rotation in the high-J limit, while $\Pi(A'')$ denotes those levels whose wavefunctions are antisymmetric. This notation has the advantage that it focuses upon the reflection symmetry of the Λ doublet level, which is the property of greatest relevance for collision dynamics. This convention can also be generalized to Δ states by writing $\Delta(A')$ and $\Delta(A'')$. The notation $\pi(\|J)$ and $\pi(\perp J)$ could be interpreted as referring to the directionality of the electron distribution in the $p\pi$ shell, or the expectation value of $\cos^2\phi - \sin^2\phi$. Unfortunately, $\langle\cos^2\phi - \sin^2\phi\rangle$ varies according to whether the $p\pi$ shell is less than or more than half filled, *i.e.* π^1 *vs.* π^3.[1] The notation $\Pi(A')$ and $\Pi(A'')$ is independent of the electron configuration of the state and applies equally, for example, to molecules in $^2\Pi$ electronic states arising from a singly filled π orbital [$CH(X^2\Pi)$ or $NO(X^2\Pi)$] and those in molecules with a π^3 electron occupancy [$OH(X^2\Pi)$ or $CN(A^2\Pi)$].

We would advocate the use of the notation $\Pi(A')$ and $\Pi(A'')$ to designate the electronic symmetry of Λ doublet levels of a Π electronic state when a concise description of this property is needed.

1 M. H. Alexander and P. J. Dagdigian, *J. Chem. Phys.*, 1984, **80**, 4325.
2 B. Pouilly, P. J. Dagdigian and M. H. Alexander, *J. Chem. Phys.*, 1987, **87**, 7118.

Dr N. C. Firth and **Prof. R. Grice** (*University of Manchester*) said: The triplet potential-energy surfaces for the $O(^3P) + HBr$ reaction have considerable formal similarity to those of the F+HBr reaction[1] as illustrated by the correlation diagram of fig. 11 for collinear O—H—Br configurations. The $O(^3P_2)$ and $O(^3P_1)$ spin multiplet states correlate with $OH(^2\Pi_{3/2}) + Br(^2P_{3/2})$ products *via* OHBr ($^3\Pi$) intermediates which present only a modest barrier *ca.* 14 kJ mol^{-1} to reaction. The $O(^3P_1)$ and $O(^3P_0)$ spin multiplet states correlate with the spin-orbit excited products $OH(^2\Pi_{1/2}) + Br(^2P_{3/2})$ *via* $OHBr(^3\Sigma^-)$ intermediates which are expected to present a much higher barrier to reaction. Consequently reaction *via* the lowest adiabatic surfaces is expected to yield products only in the ground spin-orbit states in analogy to the F+HBr reaction.[1] However, calculations on the F+HF potential-energy surface using the diatomics-in-molecules method, including spin-orbit interaction,[2] suggest that there will be a high probability

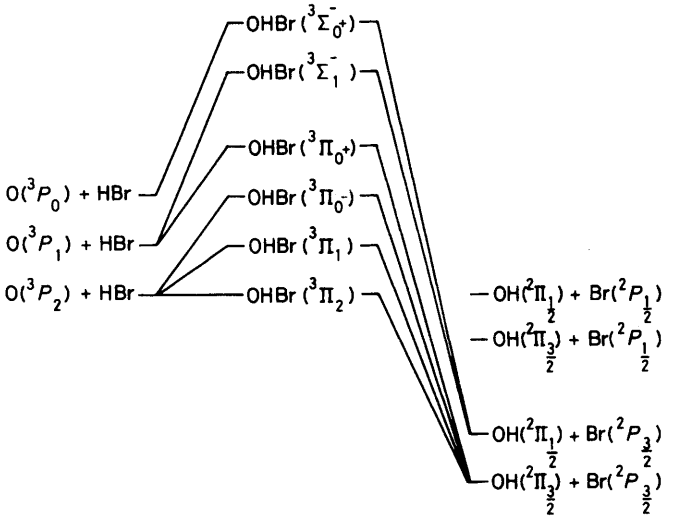

Fig. 11. Correlation diagram for triplet states of the $O(^3P)+HBr$ reaction in the collinear configuration.

of non-adiabatic transitions between the $\Omega=1, 0^+$ components of the surfaces arising from $OHBr(^3\Pi)$ and $OHBr(^3\Sigma^-)$ in the exit valley, owing to the small spin–orbit splitting of the OH radical. In the limit of strong non-adiabatic mixing for the $\Omega=1, 0^+$ components and no mixing for the $\Omega=2, 0^-$ components, a ratio 2:1 is predicted for the populations of the $OH(^3\Pi_{3/2})$ and $OH(^3\Pi_{1/2})$ spin multiplet states. This accords not only with the measurements of McKendrick *et al.*[3] but also with previous measurements of H-atom abstraction reactions of O atoms with hydrocarbon molecules,[4] where similar considerations apply to non-adiabatic transitions in the exit valley of the potential-energy surface. The measurements of Polanyi and coworkers[1,2] show a small probability of non-adiabatic transitions to the excited $Br(^2P_{1/2})$ spin multiplet state in the exit valley of the F + HBr potential-energy surface and the probability will be similarly small for $O(^3P)+HBr$. The correlation diagram shown in fig. 11 has omitted any reference to the singlet HOBr molecule, which represents the lowest potential-energy surface for this system. The energy of this surface is unknown in the OHBr configuration and the possibility of transition to the singlet surface has been ignored.

1 J. W. Hepburn, K. Liu, R. G. McDonald, F. J. Northrup and J. C. Polanyi, *J. Chem. Phys.*, 1981, **75**, 3353.
2 N. C. Firth and R. Grice, *J. Chem. Soc., Faraday Trans.* 2, 1987, **83**, 1023.
3 K. G. McKendrick, D. J. Rakestraw and R. N. Zare, *Faraday Discuss. Chem. Soc.*, 1987, **84**, 39.
4 P. Andersen and A. C. Luntz, *J. Chem. Phys.*, 1980, **72**, 5842.

Prof. A. Laganà (*University of Perugia, Italy*), **Dr F. J. Basterrechea** (*University of Pais Vasco, Spain*) and **Prof. J. M. Alvariño** (*University of Salamanca, Spain*) said: Propensity rules tying reactant orbital angular momentum ($\boldsymbol{L}$) to product rotational angular momentum ($\boldsymbol{J}'$) in halide exchanges for collisions of hydrogen halide molecules with an impinging alkali-metal atom are a distinctive feature of the light–heavy–light mass combination type. On these grounds the complexity of the computational procedure for the evaluation of the reactive cross-section of these reactions has been reduced by adopting an approach having built in a $\boldsymbol{L} \rightarrow \boldsymbol{J}'$ switch.[2] Following this approach quantum reduced dimensionality cross-sections for the H + BrH system have been calculated.[3] Recent three-dimensional quantum calculations have confirmed the reliability of the procedure.[4]

We have recently extended these techniques to the Li + HF reaction when performing a IOS calculation of the reactive cross-section.[5] For this purpose we had to make the

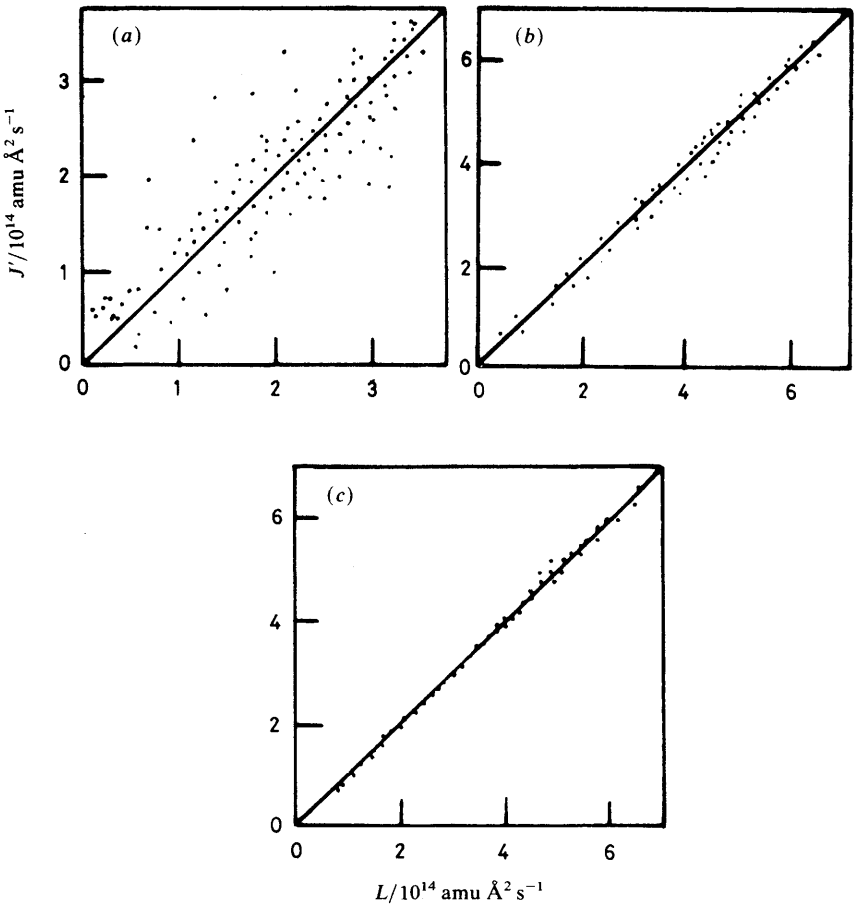

Fig. 12. Correlation diagrams of $\boldsymbol{L}$ and $\boldsymbol{J}'$ for the Li + MuF reaction calculated at a typical collision energy (15 kcal/mol) for $v = 0$ (*a*), 1 (*b*) and 2 (*c*).

mass of the central atom F *ca.* one hundred times heavier than its usual value. The factor 10 quoted in ref. (5) should read 100. Ordinate values of fig. 2 of the same reference should be multiplied by a factor of 12.75. In this way, reactant and product Jacobi coordinates are almost exactly exchangeable, and an analytical match of the entrance and exit arrangement channel wavefunctions can be applied at the dividing surface. A check for the influence of the arbitrary increase of the central atom mass on the Li + HF reactivity has been performed by comparing estimates of the quasiclassical cross-section obtained at different values of the F mass. In contrast to the blocking effect[6] found for the collinearly dominated systems, when increasing the weight of the central atom for systems having a bent transition state we obtained a small enhancement of the global reactivity.[5]

Another important dynamical constraint of the model that needed to be checked before extending the light-heavy-light computational scheme to the Li + HF reaction was the validity of the $\boldsymbol{L} \rightarrow \boldsymbol{J}'$ exchange. For this purpose we have carried out classical trajectory calculations for the Li + HF reaction and its isotopic variants. For the lightest member of this family of reactions (Li + MuF) plots of $\boldsymbol{L}$, $\boldsymbol{J}'$ pairs associated with reactive trajectories are shown in fig. 12 for the ground and the first two excited vibrational states. Correlation between initial orbital and final rotational angular momenta is fairly

good for $v=0$ and excellent for $v=1$ and 2. Similar results were obtained for heavier isotopes, although for a mass value equal to or three times larger than that of the hydrogen atom the $\boldsymbol{L} \rightarrow \boldsymbol{J}'$ correlation becomes less satisfactory.

For an extension of the light-heavy-light computational procedure to the Li + HF reaction, however, the $\boldsymbol{L} \rightarrow \boldsymbol{J}'$ exchange need not be so tight: it needs only to be enforced at the switching point between entrance and exit channels. The fact that the Li + HF system globally obeys this dynamical constraint may give an opportunity for further simplification of the computational procedure.

1 K. G. McKendrick, D. J. Rakestraw and R. N. Zare, *Faraday Discuss. Chem. Soc.*, 1987, **84**, 39; S. K. Kim, and D. R. Herschbach, *Faraday Discuss. Chem. Soc.*, 1987, **84**, 159.
2 D. C. Clary, *Mol. Phys.*, 1981, **44**, 1083.
3 D. C. Clary, *Chem. Phys.*, 1983, **81**, 379.
4 Y. Zhang, J. Z. H. Zhang, D. J. Kouri, K. Haug, D. W. Schwenke and D. G. Truhlar, to be published.
5 A. Lagana, and E. Garcia, *Chem. Phys. Lett.*, 1987, **139**, 140.
6 J. Manz, and H. H. Schor, *Chem. Phys. Lett.*, 1984, **107**, 542.

Dr T. Trickl (*University of California, CA*) and **Dr J. Wanner** (*MPQ, Garching, Federal Republic of Germany*) (*communicated*): Experiments on the $F+I_2$ reaction system exhibit the common phenomenon of visible IF chemiluminescence which varies in intensity depending upon the experimental conditions. Very weak visible IF(A-X) and (B-X) emission was observed in connection with the $F+I_2$ reaction as studied in a single-stage molecular-beam apparatus with two crossed effusive nozzles. In an earlier communication[1] we reported a first attempt at spectral resolution of the light emission associated with the $F+I_2$ system. There we attributed the spectrum to the reaction of F atoms with the trihalogen radical I_2F. The existence of this light-emitting reaction step had been verified in a molecular-beam experiment by Kahler and Lee, yet without recording a spectrum. In their experiment the trihalogen radical was formed by reaction of supersonically seeded F_2 above a distinct translational threshold energy of 17.6 kJ mol^{-1} according to: $F_2+I_2 \rightarrow I_2F+F$. This step, including the subsequent reaction of $F+I_2F \rightarrow IF+IF$, obeys bimolecular dynamics and hence proceeds as an elementary reaction.[2] We were able to extend our earlier work with a more sensitive detection system.[3] Hence at a collision energy of *ca.* 3.2 kJ mol^{-1} it was possible to obtain a vibrational product state analysis of the IF(B) state. At flows of *ca.* 2 SCCM the overall chemiluminescence signal showed a linear dependence on the iodine flow. The spectrum of the reaction $F+I_2F$ is depicted in fig. 13. Fig. 14 shows the corresponding IF(B) vibrational product state distribution. The population limit closely corresponds to the enthalpy according to $\Delta H_0^\circ = -248.5$ kJ mol^{-1}. The distribution is characterized by a 'vibrational temperature' $T_v \approx 800$ K. The latter observation is essentially identical with results of Whitehead *et al.* for a low-pressure I_2/F_2 flame,[4] where the reaction mechanism of Lee *et al.* is also anticipated. In our experiment the above reaction sequence is most likely induced by the *ca.* 5% undissociated F_2, internally excited in the microwave discharge.

1 T. Trickl and J. Wanner, *J. Chem. Phys.*, 1981 **74**, 6509.
2 C. C. Kahler and Y. T. Lee, *J. Chem. Phys.*, 1980, **73**, 5122.
3 The apparatus used is identical to the one described by M. Trautmann, J. Wanner, S. K. Zhou and C. R. Vidal, *J. Chem. Phys.*, 1985, **82**, 693.
4 D. Raybone, T. M. Watkinson and J. C. Whitehead, in *Proc. NATO Advanced Research Workshop on Selectivity in Chemical Reactions*, Bowness-on-Windermere, Sept. 1987, (Reidel, Dordrecht, in press).

Mr G. N. Robinson (*University of California, Berkeley, CA*) said: Regarding the $F+I_2$ crossed-beam results of Firth *et al.*:

(1) The relative contributions of the fast and slow $P(E')$ distributions to the IF time-of-flight spectra are not indicated in fig. 2 of their paper. How were the relative magnitudes of the forward and backward components of the CM frame angular distribution (fig. 4) determined?

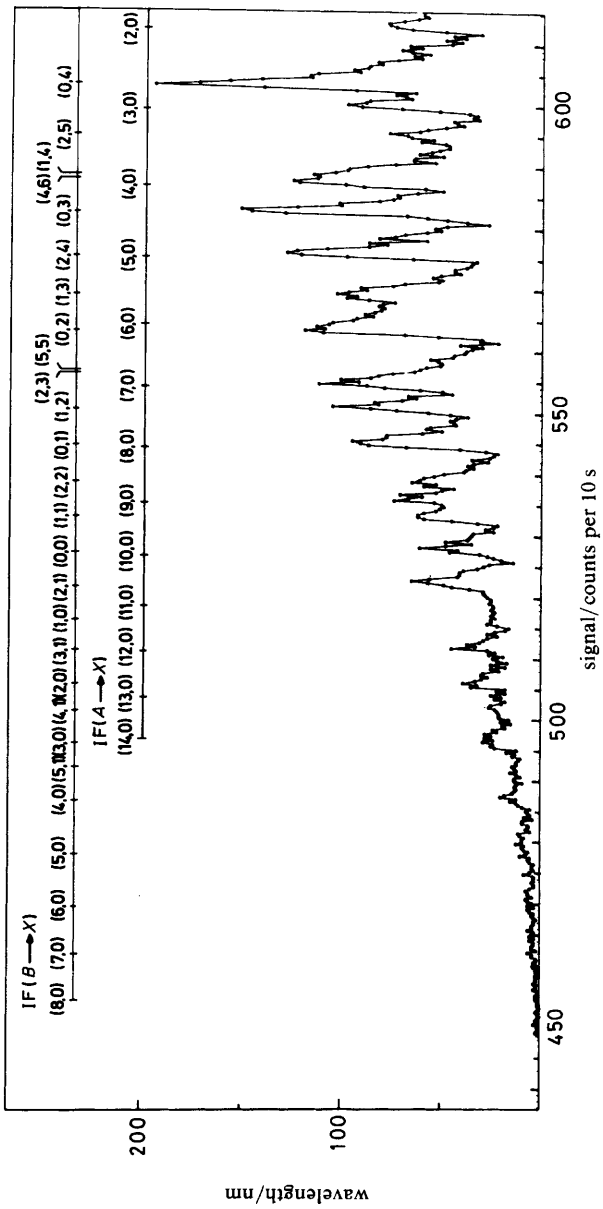

Fig. 13. Chemiluminescence spectrum of the reaction $F + I_2F$ as observed from a crossed molecular beam experiment of $F(F_2) + I_2$.

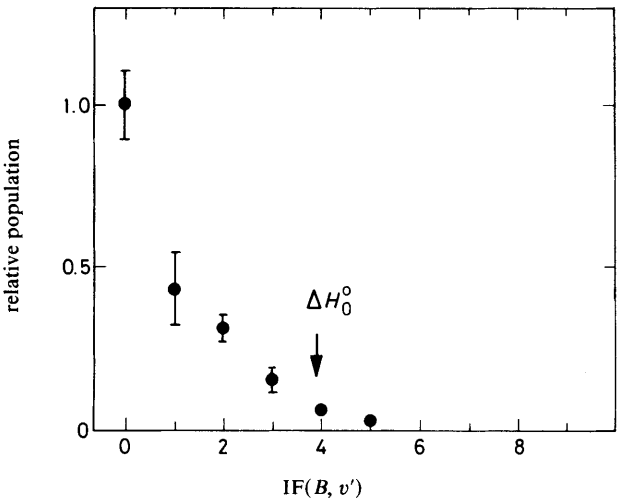

Fig. 14. The IF(B) vibrational product state distribution in agreement with results of Whitehead *et al.* for a low-pressure I_2/F_2 flame confirming the work of Kahler and Lee.[2]

(2) HIF has two stable geometries with bond angles of 137°[1a] and 87°.[1b] It is possible that FI_2 also has two stable geometries giving rise to different entrance valleys on the $F+I_2$ potential-energy surface. Could this be an explanation for the bimodal IF angular distributions?

(3) If migration were indeed important, might not intrusion of the F atom between the I atoms of I_2 promote forward and backward IF scattering as opposed to just backward scattering?

1 (*a*) R. J. Bartlett, L. Kahn and G. D. Purvis, *J. Chem. Phys.*, 1982, **76**, 731; (*b*) R. J. Bartlett, personal communication.

Dr N. C. Firth, Mr N. W. Keane, Dr D. J. Smith and **Prof. R. Grice** (*University of Manchester*) said: Comparison between the laser-induced fluorescence measurements of IF vibrational–rotational state distributions for $F+I_2$ by Girard *et al.*[1] and the differential reaction cross-section determined by Firth *et al.*[2] is not yet fully quantitative because these two experiments have been conducted at different initial translational energies and because the criteria of distinguishing two components in the reactive scattering are not identical. In order to enable a more precise description of the $F+I_2$ reaction dynamics to be formulated, further reactive scattering measurements have been undertaken using a supersonic beam of F atoms seeded in Ne buffer gas to give an initial translational energy $E \approx 19\ \text{kJ mol}^{-1}$ close to that employed by Girard *et al.*[1] Preliminary kinematic analysis yields the centre-of-mass angular distribution and product translational energy distributions for IF scattering shown in fig. 15. This shows a decrease in scattering into the backward direction which is in accord with the trajectory calculations[3] that predict a decrease in migratory trajectories at lower initial translational energy. The component of IF product scattering into the forward hemisphere with very low product translational energy has increased to a fraction *ca.* 0.15, which is in close agreement with the contribution of highly rotationally and vibrationally excited IF estimated by Girard *et al.*[1]

The trajectory calculations[3] on $F+I_2$ indicate that migratory trajectories do not give rise to precisely equal forward and backward scattering, and this is probably related to the weak transfer of angular momentum from motion of the light F atom to that of the heavy I atoms. The F atom is initially inhibited from finding a symmetrical location

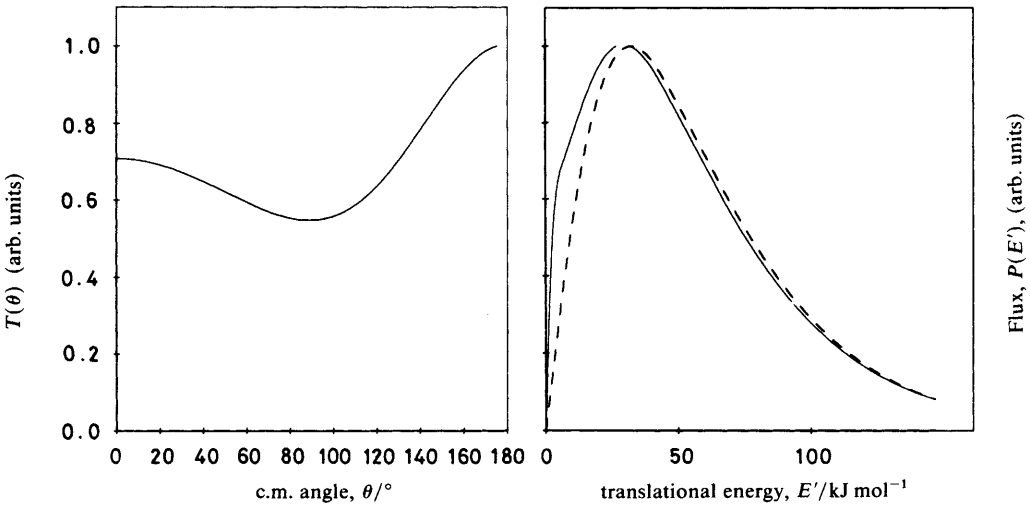

Fig. 15. Composite angular distribution and translational energy distributions for forward scattering (——) and backward scattering (- - -) for $F+I_2$ at an initial translational energy $E \approx 19$ kJ mol^{-1}.

between the two I atoms since this represents an energetically unfavourable configuration. For this reason the F atom was described as intruding rather than inserting into the I_2 bond. In view of the extensive experimental data which have now been accumulated on $F+I_2$, it will be of great interest to see whether further trajectory calculations do indicate a bent preferred geometry for FI_2 and indeed to investigate the possibility of two stable geometries as just suggested by Mr. Robinson.

1 B. Girard, N. Billy, G. Gouedard and J. Vigué, *Faraday Discuss. Chem. Soc.*, 1987, **84**, 65.
2 N. C. Firth, N. W. Keane, D. J. Smith and R. Grice, *Faraday Discuss. Chem. Soc.*, 1987, **84**, 53.
3 I. W. Fletcher and J. C. Whitehead, *J. Chem. Soc., Faraday Trans. 2*, 1984, **80**, 985.

Dr J. C. Whitehead (*University of Manchester*) said: Firth *et al.*[1] and Girard *et al.*[2] have commented on the role of migration in the reaction $F+I_2$ and have referred to the trajectory studies of Fletcher and myself[3] in which we first pointed out the importance of migration in this reaction. At the time of that study, experimental data of the quality and extent presented at this Discussion[1,2] were not available. We used an extended LEPS potential-energy surface with a well whose depth was adjusted to fit the known stability of FI_2 [4] assuming a collinear geometry. Migration in which the F atom initially attacks one of the iodine atoms and then moves round to the other was found to be common at the energies of the experiments[1,2] occurring in $>50\%$ of trajectories. The migratory trajectories were found to take place at higher impact parameters, and to have higher product recoil energy with more backward scattering, higher IF rotation (fig. 16) and lower IF vibration (fig. 17) than the direct trajectories in agreement with the interpretation of Firth *et al.*[1] In particular, note that the combination of direct trajectories giving forward scattering and an almost equal proportion of migratory trajectories that are backward scattered gives an overall appearance of symmetric forward–backward scattering that could be misinterpreted as indicating a long-lived collision complex where there is no evidence for statistical behaviour in this system. In fact it is possible that migration might occur in similar systems, *e.g.* $O+I_2$, and the assumption of a long-lived collision complex might also be incorrect.

It would be helpful to examine the rotational data of Girard *et al.*[2] and determine *via* Doppler profiles whether it is possible to associate the high J' component with

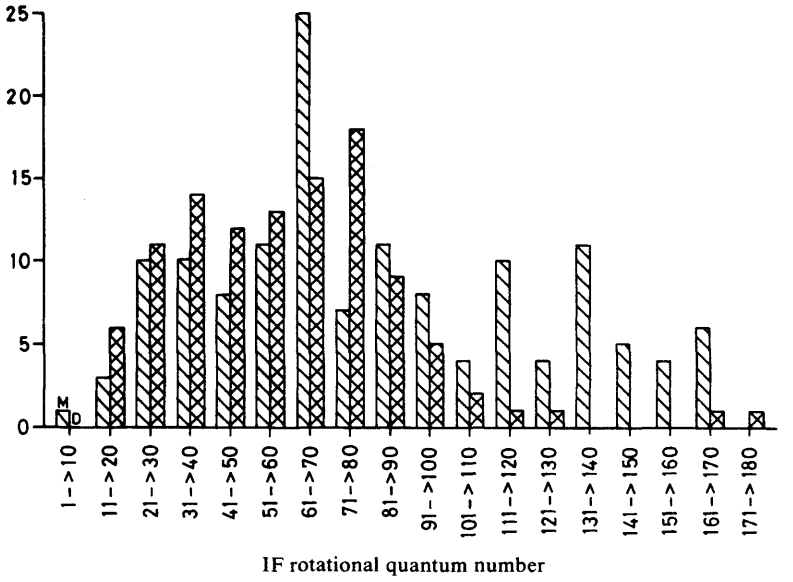

Fig. 16. The IF rotational state distribution for the reaction $F+I_2$ ($v=0$, $J=20$, $E_{trans}=8.4$ kJ mol^{-1}) → IF(J') + I for the direct trajectories (D) and migratory trajectories (M).

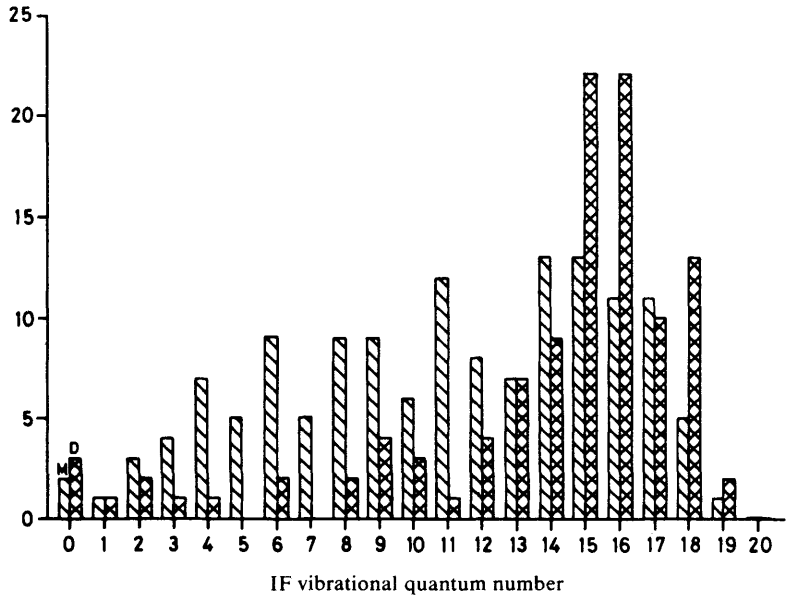

Fig. 17. The IF vibrational state distribution for the reaction $F+I_2$ ($v=0$, $J=20$, $E_{trans}=8.4$ kJ mol^{-1}) → IF(v') + I for the direct trajectories (D) and migratory trajectories (M).

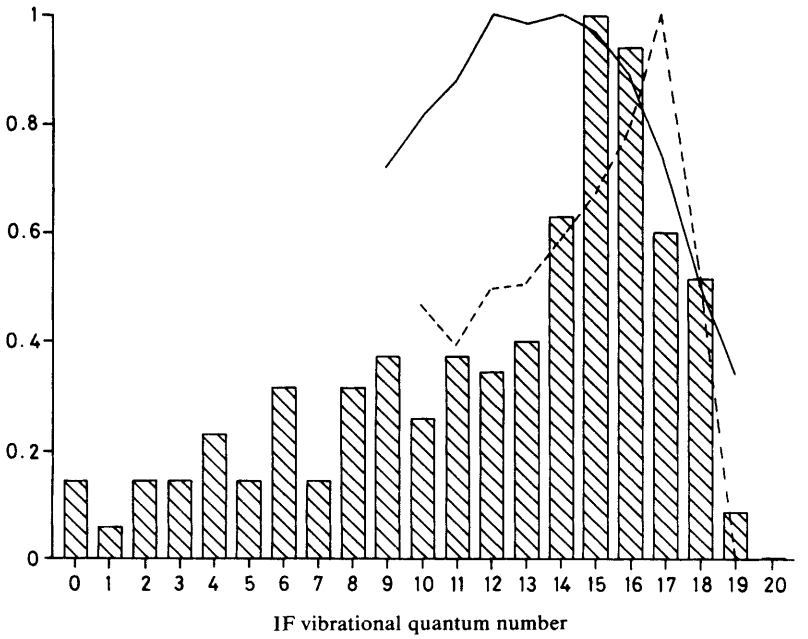

Fig. 18. The overall IF vibrational state distribution for the reaction $F+I_2$ ($v=0$, $J=20$, $E_{trans}=8.4$ kJ mol^{-1}) $\rightarrow IF_2(v')+I$ compared with the experimental results of Girard *et al.*[2] (——) and of Trickl and Wanner[5] (- - -).

higher recoil velocity and the low J' component with lower product recoil energy, and thereby confirm the characteristics of migratory collisions. The comparison of the overall computed IF(v') vibrational distribution with the determinations of Girard *et al.* and Trickl and Wanner[5] (fig. 18) shows that there is still a need to establish a definitive vibrational distribution. It is now clear that the LEPS surface used in the trajectories is incorrect in the geometry of the FI_2 intermediate, which should be bent,[1] but that it is correct in having dominant long-range attraction. Given the improved data now available, we should be able to derive a surface of greater accuracy and hopefully improve agreement with experiment.

1 N. C. Firth, N. W. Keane, D. J. Smith and R. Grice, *Faraday Discuss. Chem. Soc.*, 1987, **84**, 53.
2 B. Girard, N. Billy, G. Gouedard and J. Vigué, *Faraday Discuss. Chem. Soc.*, 1987, **84**, 65.
3 I. W. Fletcher and J. C. Whitehead, *J. Chem. Soc., Faraday Trans. 2*, 1984, **80**, 985.
4 J. J. Valentini, M. J. Coggiola and Y. T. Lee, *J. Am. Chem. Soc.*, 1976, **98**, 853.
5 T. Trickl and J. Wanner, *J. Chem. Phys.*, 1983, **78**, 6091.

Mr B. Girard, Dr N. Billy, Dr G. Gouédard and **Dr J. Vigué** (*Université Paris VI, France*) replied: In his comment, Dr Whitehead points out that the vibrational distribution of IF produced by the $F+I_2$ reaction is not firmly established, as the results of Trickl and Wanner[1] are not in good agreement with ours. We will show that this discrepancy can be explained as being due to the analysis of the laser-induced fluorescence spectrum made by Trickl and Wanner. This analysis[2] was based only on bandhead intensity measurements and was not sensitive to the high-J part of the rotational distribution. In order to give further support to this idea, we have calculated truncated vibrational densities from our data:

$$n_{J_0} = \sum_{J=0}^{J_0} n(v, J).$$

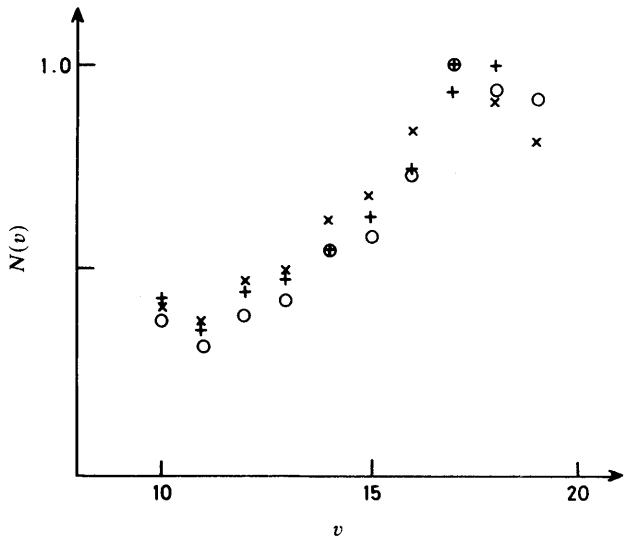

Fig. 19. Comparison between vibrational densities: + $n(v)$, Trickl and Wanner;[1] ○, $n_{25}(v)$, this work; ×, $n_{50}(v)$, this work.

We have taken $J_0=25$ and 50, and fig. 19 presents plots of these quantities, $n_{25}(v)$ and $n_{50}(v)$ as a function of v, together with the measurements of Trickl and Wanner.[3] These three sets of points (which have been normalized at their maximum values) present exactly the same vibrational dependence. This proves directly that the difference of $n(v)$ between our results[4] and those of Trickl and Wanner[1] is entirely due to the high-J contribution to $n(v)$. Whether this high-J part of the rotational distribution was produced in the experiment of Trickl and Wanner and neglected in the analysis of the spectrum, or not produced because the collision energy in their experiment is lower than in ours, is a point which remains to be settled.

Finally, the conversion from density to flux remains to be made, in order to make a direct comparison with the results of trajectory calculations. This conversion requires some knowledge of the differential cross-sections that we want to get from a study of Doppler lineshapes. Furthermore, this information should reveal finer details on the bimodal character of the collision dynamics.

1 T. Trickl and J. Wanner *J. Chem. Phys.*, 1983, **78**, 6091.
2 J. Wanner, personal communication (1987).
3 By a reading of Dr Trickl's thesis we have found that there is a misprint in ref. (1); the value of n ($v=18$) should read 2.06 ∓ 0.18.
4 B. Girard, N. Billy, G. Gouédard and J. Vigué *Faraday Discuss. Chem. Soc.*, 1987, **84**, 65.

Mr K. Wagemann and **Dr J. Wanner** (*MPQ, Garching, Federal Republic of Germany*) and **Prof. X. K. Zeng** (*Dalian Institute of Chemical Physics, China*) said: In their paper as well as in a recent publication, Vigué *et al.* give proof that almost all of the intense IF($v=0$) population so far observed in the laser-induced fluorescence studies of the $F+I_2$ reaction system does not result from the elementary gas-phase reaction but probably originates from a surface process releasing IF molecules with a sub-Doppler velocity profile.[1] This conclusion is confirmed in the paper by Grice and co-workers.[2]

In search of clarification we re-investigated the $F+I_2$ and F+ICl systems in an experimental variant in which the reaction was carried out in a concentric discharge-flow reactor at very low reagent flows, the iodides being diluted in He. The quartz flow tube was incorporated into the cryo-pumped and cold-shielded reaction vessel which was

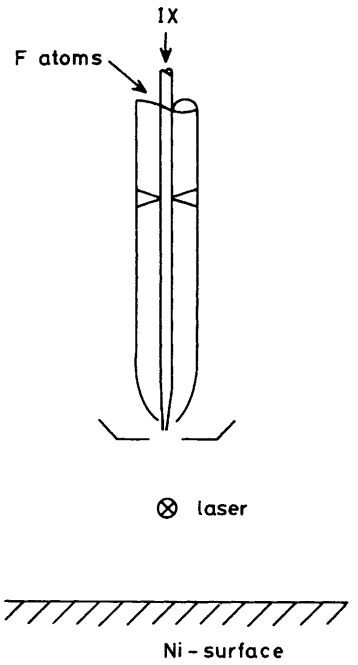

Fig. 20. Arrangement of discharge-flow reactor, surface and dye laser as used to confirm the existence of a surface reaction, generating IF($v=0$) molecules in reactions of F atoms with condensed IX (X = I, Cl).

used earlier in connection with two effusive beams.[3] In both reactions pronounced bimodal IF product state distributions were again obtained, with similar branching ratios as reported earlier.[3] Under these conditions, where the products are presumably closer to translational equilibrium, the population distributions of levels $v \geq 2$ as ascribed to the elementary gas-phase reaction were found to be essentially identical as reported in ref. (3).

In addition, the flow tube in conjunction with a nickel surface mounted at a distance of 3 cm and maintained at a controlled temperature allows one to verify the participation of a surface reaction. The arrangement is depicted in fig. 20. Nickel was chosen, since it is the material of the inner reaction vessel normally maintained at liquid-nitrogen temperature. Hence the flux of products emerging from the reactor together with the remaining reagents, mainly fluorine atoms and molecular iodine, was directed onto the surface and the IF density was monitored with laser-induced fluorescence. At elevated temperatures a strong signal increase by surface-enhanced generation of IF ($v=0$) molecules was noticed. For $F+I_2$ this effect disappears at a characteristic threshold temperature of $T_s = 200$ K. Below this temperature (as seen in fig. 21) only those small amounts of IF($v=0$) molecules are detected which are already produced in the flow reactor. The rotational product state analysis of the surface-generated molecules shows that these are in equilibrium with the surface over the full range of temperatures used. In order to prove that the surface selectively enhances the $v=0$ populations, the experiment was repeated by monitoring several high vibrational product levels. As shown in fig. 21 for $v=14$, for example, no signal enhancement was measured within the experimental error limits. Hence we confirm the existence of a surface reaction which releases equilibrated IF($v=0$) molecules into the gas phase. Since this effect disappears when the microwave discharge is switched off, we ascribe it, in agreement with the observations of Grice *et al.*, to the reaction of F atoms with condensed iodine.

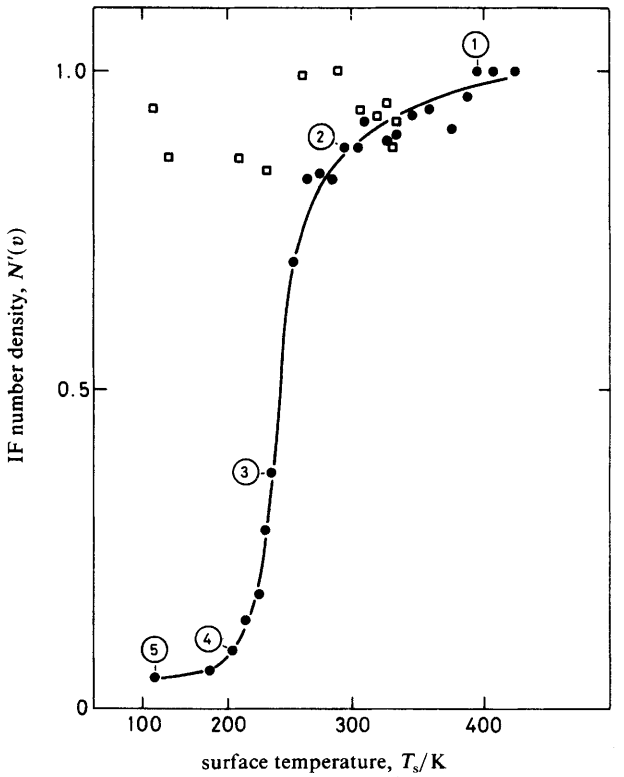

Fig. 21. The generation of rotationally equilibrated IF($v=0$) molecules in the F+I_2 reaction at the surface exibits a distinct threshold behaviour (●). The small amount of products detected below the threshold temperature stems from the wall reaction at the flow tube exit. High vibrational IF product states are unaffected by the surface, as depicted, for example, for IF($v=14$) (□). T_{rot}/K = (1) 360, (2) 280, (3) 220, (4) 180 and (5) 270.

We also found that this process depends linearly on the F atom flow. The same dependence for IF($v=0$) was noticed in our crossed-beam experiments.[3] Apart from the observation of sub-Doppler linewidths and the verification of single collision conditions, this behaviour led to the belief that the $v=0$ branch of population originates from bimolecular gas-phase dynamics.

Note that we also carried out an additional experiment in which a layer of I_2 was first condensed onto the surface and subsequently exposed to the impinging F atoms. Here again IF($v=0$) molecules, rotationally equilibrated with the surface, were released at the same threshold temperature as reported above.

For the F+ICl system there is a similar effect, which, however, is too large to be explained in terms of the small amount of residual I_2 in ICl (*ca.* 0.1%[3]). The proof of a less efficient surface reaction of F atoms with condensed ICl was obtained by observation of a different, distinct threshold temperature $T_s = 170$ K.

The rotational analysis of the surface reaction products presents an unambiguous criterion as to where the $v=0$ contributions in our product-state distributions originate. These locations are the warm walls close to the prereactor tip, and, in the crossed-beam experiments, the iodine nozzle maintained at 350 K.

On the basis of the rotational distribution we can also determine the existence of real IF($v=0$) populations to be due to the gas-phase reactions. For the F+I_2 reaction

a rather small contribution was established in the flow-tube experiment. According to a rotational fit of the excitation spectrum this population corresponds to a temperature much greater than that of the prereactor walls, $T = 270$ K. On the other hand, for F + ICl there is a population of the IF($v = 0$) level at $T_r = 2750$ K. This contribution is more significant as already noted in our crossed-beam work.[3]

1 B. Girard, N. Billy, G. Gouédard and J. Vigué, *Faraday Discuss. Chem Soc.*, 1987, **84**, 65; *Chem. Phys. Lett.*, 1987, **136**, 101.
2 N. C. Firth, N. W. Keane, D. J. Smith and R. Grice, *Faraday Discuss. Chem. Soc.*, 1987, **84**, 53.
3 T. Trickl and J. Wanner, *J. Chem. Phys.*, 1983, **78**, 6091.

Dr N. C. Firth, Dr D. J. Smith and **Prof. R. Grice** (*University of Manchester*) said: The description of the surface reaction of F atoms and I_2 molecules is in accord with our previous experience when studying the F + ICl and F + I_2 reactions[1,2] in a crossed-beam experiment using a mass spectrometer detector. During initial experiments IF was observed at a very low laboratory velocity, which was kinematically inconsistent with IF product scattering arising from reactive collisions in the scattering centre. Indeed this background signal was removed immediately upon flagging the F atom beam but decayed only slowly after flagging the ICl or I_2 molecule beam. It was therefore concluded that this signal arose from the reaction of F atoms with I_2 molecules adsorbed on warm surfaces lying within the field of view of the mass spectrometer detector. Consequently all such surfaces were clad with Cu shielding cooled to *ca.* 100 K, and this removed the background IF signal. The product translational energy distribution for the F + ICl reaction[1] was compared with that predicted from the IF vibrational and rotational state distributions of Trickl and Wanner.[3] Good agreement was obtained[1] for IF vibrational states other than $v = 0$ or 1 and it was concluded that the intensity of the laser-induced fluorescence signal observed by Trickl and Wanner for these levels arose from surface reaction which could not readily be distinguished from crossed-beam scattering in the absence of the kinematic discrimination provided by time-of-flight measurements.

1 N. C. Firth, D. J. Smith and R. Grice, *Mol. Phys.*, 1986, **61**, 859.
2 N. C. Firth, N. W. Keane, D. J. Smith and R. Grice, *Faraday Discuss. Chem. Soc.*, 1987, **84**, 53.
3 T. Trickl and J. Wanner, *J. Chem. Phys.*, in press.

Mr B. Girard, Dr N. Billy, Dr G. Gouédard and **Dr J. Vigué** (*Université Paris VI, France*) added: In their comment, Dr Wanner and Mr Wagemann have presented nice experimental results showing that the IF($v = 0$) molecules are due to a wall reaction. These confirm our result[1] that the IF($v = 0$) molecules are not a direct product of the F + I_2 gas-phase reaction. We thus agree on this point and we wish to present further evidence of its correctness.

The first piece of information comes from the Doppler lineshapes: the $v = 0$ lines were found to be very narrow in our experiment,[1] corresponding to an apparent temperature of <100 K. This value could not be explained by the wall temperature, as it remained unchanged even when all the walls were kept at room temperature. On the other hand, this feature is easily understood as due to the following collimation effect: the IF($v = 0$) molecules are produced by wall reactions in the vicinity of the F beam and they can be detected only if they fly towards the scattering centre; this selects their velocity as almost parallel to the F beam and perpendicular to the laser beam.

The second item of information comes from the fact that the $v = 0$ signal is strongly enhanced (typically by a factor of 5) if the F beam is flagged in the scattering chamber, before the scattering centre. In this case all the fluorine atoms diffuse to the walls where they react, whereas only a small fraction of the unflagged beam can strike a wall.

We consider that these results prove clearly that the IF($v = 0$) molecules observed are not due to the direct reaction of F + I_2 but to a wall reaction. We have tried to detect

$v = 0$ molecules due to the direct reaction. These efforts have been unsuccessful even when working at large J values (near $J = 80$ and 120), where the signal coming from the wall reaction is negligible. However, the upper limit we can fix to the density of $v = 0$ molecules is not very low: $n(v = 0) \leqslant n(v = 13)$. This is due to the fact that, if the iodine atom is in its $^2P_{3/2}$ ground state, many levels can be populated in $v = 0$ (up to $J \approx 200$), and there is a good deal of recoil energy available for the lower J values, implying very broad Doppler line profiles.

1 B. Girard, N. Billy, G. Gouédard and J. Vigué, *Chem. Phys. Lett.*, 1987, **136**, 101.

Prof. A. Laganà (*University of Perugia, Italy*) and **Dr L. A. M. Quintales** and **Prof. J. M. Alvariño** ((*University of Salamanca, Spain*) said: The dynamical behaviour of the H + ICl reaction has been taken as a model for rationalizing the reactivity of systems involving halogen-containing molecules. The H + ICl reaction was first investigated by Polanyi and co-workers.[1] In their study evidence was given for the possibility of obtaining the HCl product even when H first impinges and binds to the I atom. Recently we have reinvestigated this reaction using the same potential-energy surface and the same set of initial conditions. In addition, calculations were also carried out at higher collision energy (T) as well as at different initial orientations of the target diatom in order to provide evidence of stereospecific properties of this reaction.

A basic feature of the H + ICl reactivity is the competition between Cl and I for forming the product hydrogen halide. Our results agree with the findings of Polanyi and co-workers of a strong preference of the reaction for the HI product at low collision energy. However, we also find that this bias is less pronounced at higher energies. This effect can be attributed mainly to a competition between two direct (collinearly dominated) mechanisms. The typical behaviour of direct collinear reactive probabilities [$P(E)$] is illustrated in fig. 22. In the upper panel (for systems such as H + I with no barrier to reaction) $P(E)$ is fully reactive at low collision energies as a result of the fact that the potential is attractive from long-range inward. At higher T values $P(E)$ decreases. On the LEPS surface adopted for the H + ICl reaction, this can be understood in terms of back reflection from the wall opposite to the entrance channel. In fact, once the collision energy is large enough to allow reflected trajectories to return to the reactant asymptote, a further increase in T lowers the reactive probability (*i.e.* the complement to one of the fraction of back-reflected trajectories).[2] The lower panel shows the case of reactions having (like H + Cl_2) an early barrier. For systems having an early barrier to reaction there is first a reflection at low collision energy occurring at the bottleneck associated with the saddle. At higher collision energies $P(E)$ increases to reach (possibly) full reactivity. At even higher T values the amount of energy in excess of the height of the saddle becomes larger, and back reflection can start to occur. Because of this, the tail of the $P(E)$ curve for these systems decreases, as in the case of reactions without a barrier.

A more composite mechanism is followed by other reactive collisions.[3] If the reactive path goes through a situation in which insertion almost occurs, a non-negligible fraction of trajectories can spend a certain amount of time in finding the final exit. In this case, migration from the atom of the first attack to that forming the product diatom is likely to occur. Migration of H from I to Cl has been singled out in ref. (1). The graphical study performed on our trajectories shows that at first H binds to I after being captured from its long-range attractive tail. Then, while ICl stretches, H passes around the I atom, undergoing several hindered rotations (see fig. 23) till the moment it finds a location for which the barrier to react with Cl is small.

Our calculations, however, have also shown the possibility that collisions starting on the Cl side lead to the formation of HI. In this case (fig. 24) the hydrogen atom binds at first with the nearest atom (Cl), around which it performs a few oscillations. When it reaches a favourable location, capture by the iodine atom is possible.

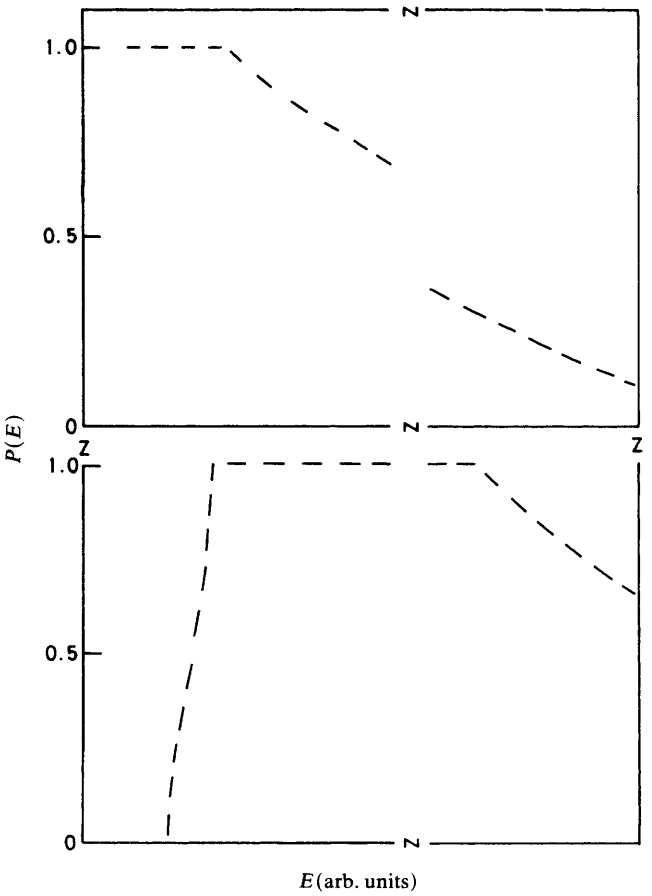

Fig. 22. Qualitative evolution with energy of reactive collinear probability for systems with a barrier to reaction (lower panel) and systems with no barrier (upper panel).

Finally, a case less likely to occur is that of H orbiting for a while around the ICl molecule before reacting with either I or Cl. This type of floppy aggregate, stabilized by rotational trapping around the target molecule, has been found to be more effective in promoting the release of internal energy in non-reactive processes[4] rather than those leading to reaction.

1 J. C. Polanyi, J. L. Schreiber and W. J. Skrlac, *Faraday Discuss. Chem. Soc.*, 1979, **67**, 66.
2 J. N. L. Connor and A. Laganà, *Mol. Phys.*, 1979, **38**, 657.
3 J. M. Alvariño and A Laganà, *J. Phys. Chem.*, 1987, **97**, 5487.
4 J. P. Tosi, M. Ronchetti and A. Laganà, *J. Chem. Phys.*, 1988, in press.

Dr M. R. Levy (*Newcastle-upon-Tyne Polytechnic*) said: Prof. Polanyi[1] has referred to the novel technique of laser ablation for producing atomic beams, and Costes *et al.*[2] have admirably demonstrated its application to the study of aluminium atom reactions. As a further illustration of the potential of this approach, I would like to present some results from recent work on transition-metal atom reactions.[3] Experiments in this area have the potential to be particularly rewarding, since both the metal atoms and the diatomic oxide or halide product molecules have many low-lying electronic states (some metastable), so that a large number of potential surfaces may interact. Laser ablation

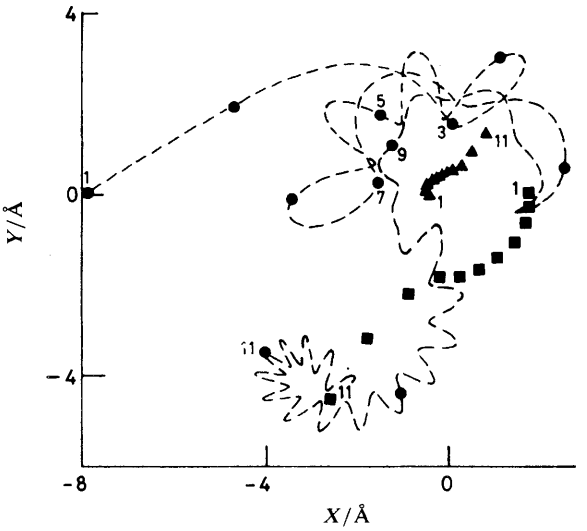

Fig. 23. A daisy plot of a reactive trajectory showing the migration of H from I to Cl. The positions of H (●), I (▲) and Cl (■) after identical intervals of time are labelled by the same number.

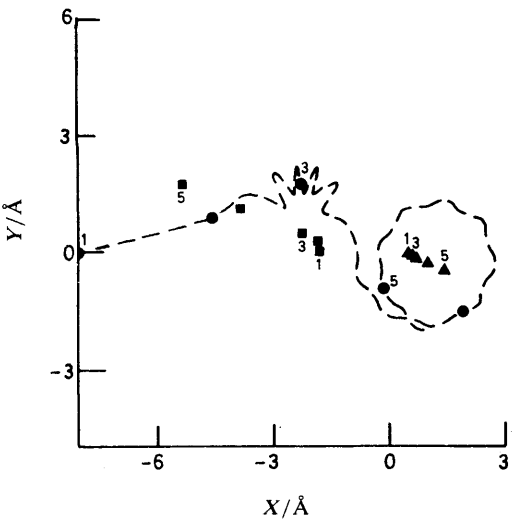

Fig. 24. As in fig. 23 for the migration of H from Cl to I.

is especially appropriate in view of the high refractivity of the metals, which has restricted previous dynamical investigations to a relatively small number.[4]

My own studies have concerned chemiluminescent reactions of the type

$$Mn + RO \rightarrow MnO^*(A\,^6\Sigma^+) + R$$

(R = O, N_2, CO, NO). This represented a suitable starting point for studies of transition-metal atom reactions because of the relative simplicity of (*a*) the Mn electronic structure (fig. 25)[5] and (*b*) the well known $MnO(A\,^6\Sigma^+ - X\,^6\Sigma^+)$ spectrum from *ca.* 450 to *ca.* 750 nm.[6] Fig. 26 shows the experimental arrangement. There are two important

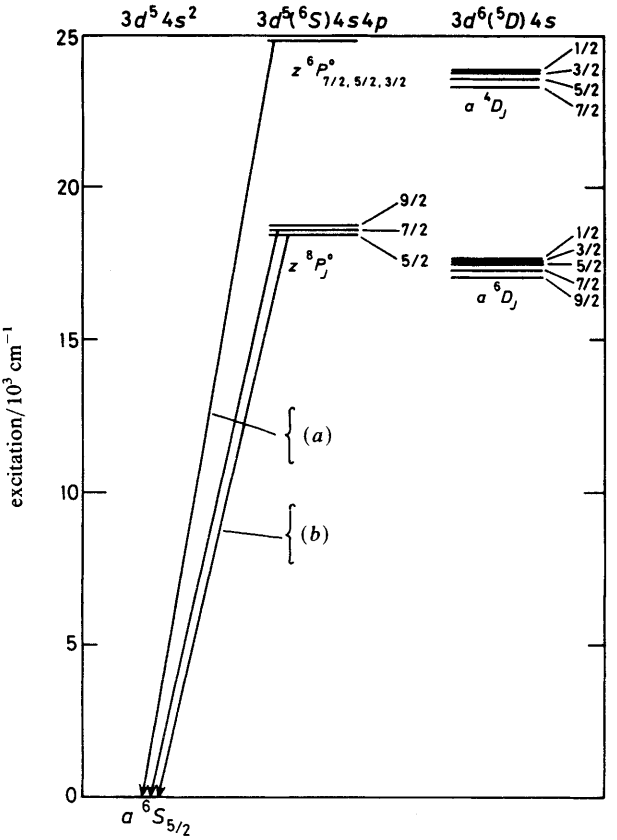

Fig. 25. Low-lying electronic structure of the Mn atom.[5] The $a\,^6D_J$ and $a\,^4D_J$ states are truly metastable. (*a*) $\lambda = 403.1$, 403.3 and 403.5 nm; $\tau \approx 50$ ns. (*b*) $\lambda = 539.5$ and 543.5 nm; $\tau \approx 80$ and 120 μs.

differences from that used by Costes *et al.*[2] First, a beam-gas configuration was employed; secondly, the metal target was ablated in the absence of any carrier gas from a pulsed valve. In this approach, devised by Kang and Beauchamp,[7] the laser is focussed onto the target by a concave mirror placed in front of it, and the pulsed atomic beam passes out through a narrow hole in the centre of the mirror. The predominant ionic component in the beam is deflected away by a d.c. electric field. While this technique does not give the narrow velocity spread and high peak intensities achievable with pulsed valves, it does offer some advantages: it is relatively simple; the broad velocity spread is immediately resolvable by time-of-flight analysis, so that excitation functions can be measured; the velocity distribution can be altered by adjusting the laser focussing; and the temperature of the laser-induced plasma is so high that the beam contains a substantial proportion of atoms in metastable states. In addition, in the case of Mn, the beam can be detected by the long-lived emission at *ca.* 540 nm from the $^8P_{7/2,5/2}$ levels ($\tau = 83 \pm 10$, 123 ± 14 μs, respectively.[3]

The collimated beam and its reaction with oxidiser molecules were monitored optically at a point 283 mm from the target. Data were time-of-flight spectra of the beam number density (weighted by the exponential decay of the ^8P levels), and the corresponding time-dependent emissions produced when oxidiser was admitted to the scattering chamber. Between 64 and 1024 laser shots were averaged, depending on what

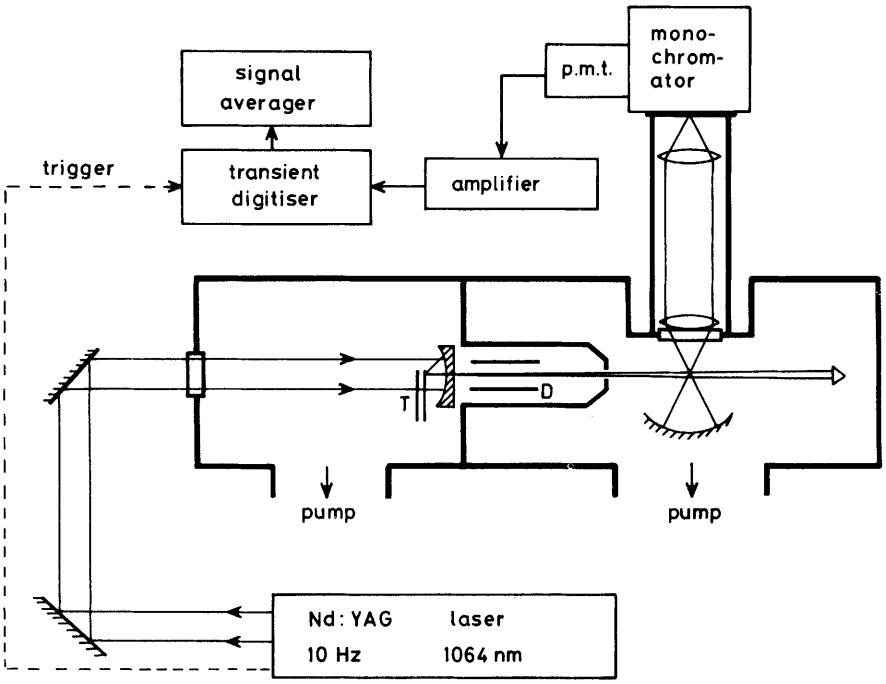

Fig. 26. Schematic of experimental arrangement. T, target; D, ion deflection plates.

was being observed. Fig. 27 shows a typical time-profile of the metastable emission, $P(t)$, together with the corresponding Mn *flux* distribution, $N'(t)$ (including the correction for the metastable decay). The beam velocity ranges from >2000 to $<20\,000$ m s^{-1}, and the distribution in fig. 27 can be characterised by a plasma temperature of *ca.* 77 000 K.[3] The metal atom beam velocity determines the mean collision energy; and, for the bulk of the velocity range, the oxidiser velocity is negligible.

MnO*($A\,^6\Sigma^+$) chemiluminescence was observed when O_2, CO_2, N_2O or NO_2 was admitted to the scattering chamber. The pressure dependence was linear up to *ca.* 0.020 Pa (*ca.* 1.5×10^{-4} Torr), indicating first-order kinetics. Collision-induced atomic emission was also detected at *ca.* 403 nm, due to either the $z\,^6P^0 \rightarrow a\,^6S$ or $z\,^6D^0 \rightarrow a^6D$ transitions of Mn. Fig. 28(*a*) shows typical time profiles, $I(t)$, of both the MnO* emission ($\lambda > 550$ nm) and the collision-induced Mn* emission from Mn + N_2O. As the radiative lifetimes of these emissions are short, $I(t)$ measures flux and can be readily converted into $\sigma(E_T)$, the relative cross-section at the translational energy E_T corresponding to the time-of-flight t, by dividing by $N'(t)$.

The resulting excitation functions for the two emissions from Mn + N_2O are shown in fig. 28(*b*) It is noticeable that the fall-off in the molecular emission is matched by the rise in the atomic signal. The arrows on the E_T axis indicate the thresholds for MnO*(A)[6,8] and Mn*($z\,^6P^0$)[5] production from Mn($a\,^6S$). Although there is some noise in the data, the figure strongly suggests that $a\,^6S$ atoms, rather than $a\,^6D$ or higher states, are the species responsible for both processes, and that the 403 nm emission is $z\,^6P^0 \rightarrow a\,^6S$, rather than $z\,^6D^0 \rightarrow a\,^6D$. In fact the threshold for MnO* production indicates a barrier *ca.* 70 kJ mol^{-1} above the endoergicity; the barrier for $a\,^6D$ atoms must therefore be even higher. This contrasts with Mn + O_2, CO_2 and NO_2,[3] where both MnO*(A) and Mn*($z\,^6P^0$) derive, at least in part, from excited $a\,^6D$ atoms, but where the MnO* threshold is equal to the endoergicity. However, in these cases too, the

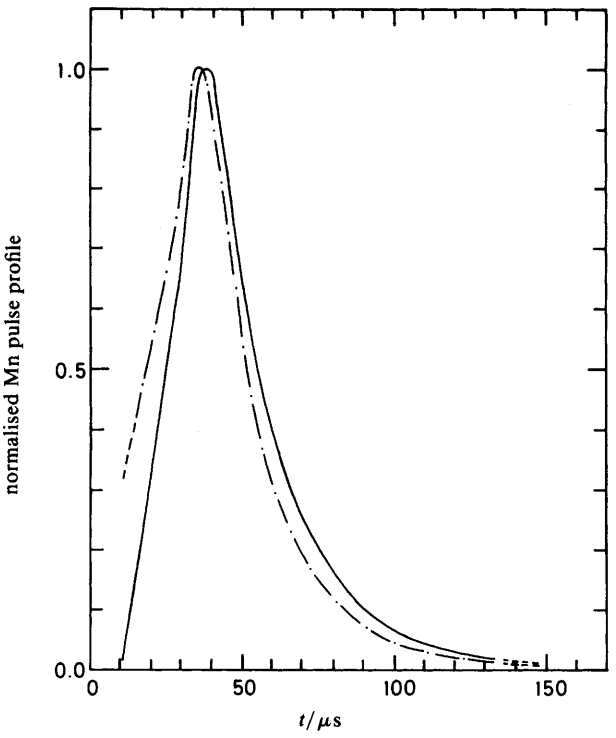

Fig. 27. Typical time profile of Mn*(^8P) emission, $P(t)$, monitored at 283 mm from the target (——), together with the corresponding derived time-profile of the non-emitting Mn atom flux, $N'(t)$ (— · —).

reactivity seems largely restricted to Mn($a\,^6S$, $a\,^6D$), despite the undoubted presence in the beam of even higher metastable states.

Adiabatic correlation diagrams can go some way towards explaining the behaviour of these reactions.[3] In most cases they suggest that $a\,^6S$ atoms should lead to MnO(X), whereas MnO*(A) should derive largely from $a\,^6D$ atoms. Nonetheless, ground-state Mn atoms could still give MnO*(A) through intersystem crossing in the collision complex, if it lives long enough, or through overlap between the X- and A-state vibrational manifolds. The replacement of MnO* by Mn*($z\,^6P$) with increasing E_T, in Mn + N_2O, suggests that the collision complex lives long enough for crossover to occur between the surfaces corresponding to Mn($a\,^6S$) and Mn*($z\,^6P$).

Correlation diagrams, however, give little information about potential barriers. It is conceivable that the large excess barriers for reaction of both Mn($a\,^6S$ and $a\,^6D$) with N_2O arise from the high second ionisation potential of Mn; but this does not explain the different behaviour in the isoelectronic Mn + CO_2. Potential barriers have been noted previously in the reaction of a number of metals with N_2O, *e.g.* Na[9] and Sn,[10] but there have been relatively few comparative studies of N_2O and CO_2 reactions (probably because the latter are mostly endothermic). In their paper, Costes *et al.*[2] show that Al + CO_2 has no barrier above the endothermicity; it would be interesting to learn whether Al + N_2O, *ca.* 345 kJ mol^{-1} exothermic,[2,8] does have a barrier. The energy released should be enough to populate AlO($B\,^2\Sigma^+$); however, a preliminary report elsewhere[11] indicated only weak $A\,^2\Pi$ emission under single-collision conditions.

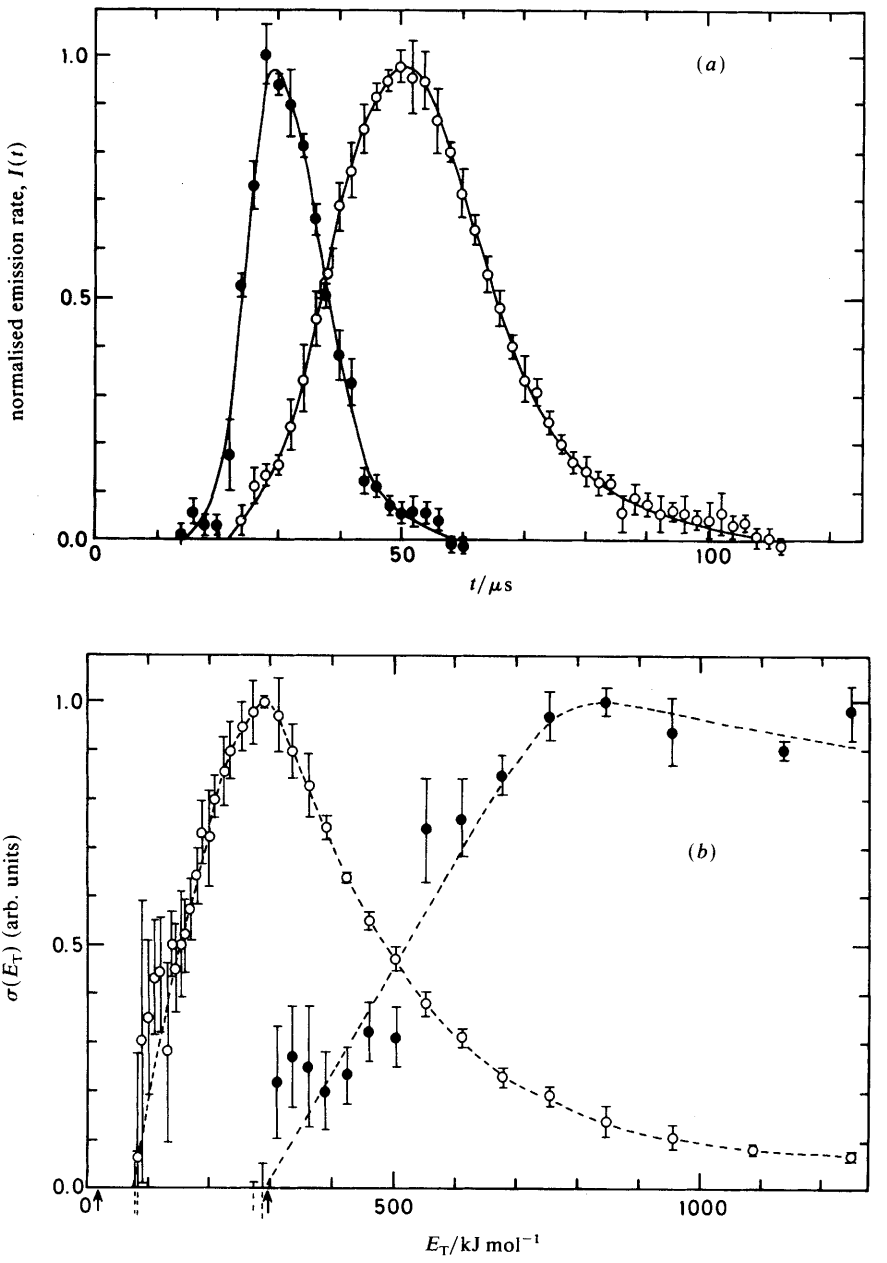

Fig. 28. (*a*) Typical time profiles of MnO*($A\,^6\Sigma^+$) (○) and Mn*($z\,^6P^0 \rightarrow a\,^6S$ or $z\,^6D^0 \rightarrow a\,^6D$) (●) emission from Mn + N_2O; (*b*) excitation functions derived from the data. The arrows on the abscissa mark the thresholds for MnO*(*A*) and Mn*($z\,^6P^0$) from Mn($a\,^6S$) (*ca.* 19 and 297 kJ mol^{-1}, respectively).

1 J. C. Polanyi, *Faraday Discuss. Chem. Soc.*, 1987, **84**, 1.
2 M. Costes, C. Naulin, G. Dorthe, C. Vaucamps and G. Nouchi, *Faraday Discuss. Chem Soc.*, 1987, **84**, 75.
3 M. R. Levy, to be published; equipment loans from the SERC Central Laser Facility are gratefully acknowledged.
4 For a rather dated review, see M. R. Levy, *Prog. React. Kinet.*, 1979, **10**, 1.
5 J. Sugar and C. Corliss, *J. Phys. Chem. Ref. Data*, 1985, **14**, suppl 2, 338 ff; S. M. Younger, J. R Fuhr, G. A. Martin and W. L. Wiese, *J. Phys. Chem. Ref. Data*, 1978, **7**, 591ff.
6 J. M. Das Sarma, *Z. Phys.*, 1959, **145**, 98; K. C. Joshi, *Spectrochim. Acta*, 1962, **18**, 625; R. M. Gordon and A. J. Merer, *Can. J. Phys.*, 1980, **58**, 642.
7 H. Kang and J. L. Beauchamp, *J. Phys. Chem.*, 1985, **89**, 3364.
8 G. Herzberg, *Electronic Spectra of Polyatomic Molecules*, and K. Huber and G. Herzberg, *Constants of Diatomic Molecules* (Van Nostrand, London, 1966 and 1979).
9 J. Pfeifer and J. L. Gole, *J. Chem. Phys.*, 1984, **80**, 565.
10 J. R. Wiesenfeld and J. M. Yuen, *Chem Phys Lett.*, 1976, **42**, 293.
11 J. L. Gole and G. J. Green, cited in S. B. Oblath and J. L. Gole, *Combust. Flame*, 1980, **37**, 293.

Dr M. Costes, Dr C. Naulin and **Dr G. Dorthe** (*University of Bordeaux, France*) said: We have indeed performed some experiments on the exoergic $Al+N_2O$ reaction. However, we have not obtained quantitative results.[1] LIF signals of $AlO(X\,^2\Sigma^+)$ remained low even at a collision energy of 0.52 eV. We also failed to detect by LIF any electronically excited $AlO(A\,^2\Pi_i)$ product, by excitation on B–A transitions on the $\Delta v=+2$ sequence near 580 nm and collecting the fluorescence of B–X transitions. Combined factors are certainly responsible for the low LIF signals: the spread of the products on the large manifold of accessible rovibrational states, the high recoil velocities which lower the densities in the laser-probed volume, and perhaps a lower reactive cross-section than for the other reactions. We have not made runs under 0.30 eV collision energy and thus cannot conclude about the existence of an energy barrier. This eventuality seems, however, very likely, as it is often the case for atom–nitrous oxide reactions. For example, we have observed an energy barrier for the exoergic $C+N_2O$ reaction.[2]

1 M. Costes, C. Naulin, G. Dorthe and G. Nouchi, in *NATO Advanced Research Workshop on Selectivity in Chemical Reactions*, ed. J. C. Whitehead (Reidel, Dordrecht, 1988).
2 M. Costes, G. Dorthe, B. Duguay, P. Halvick, J. Joussot-Dubien, C. Naulin, G. Nouchi, J. C. Rayez, M. T. Rayez and C. Vaucamps, in *Recent Advances in Molecular Reaction Dynamics*, ed. R. Vetter and J. Vigué (C.N.R.S., Paris, 1986), p. 97.